CHALMERS
UNIVERSITY OF TECHNOLOGY

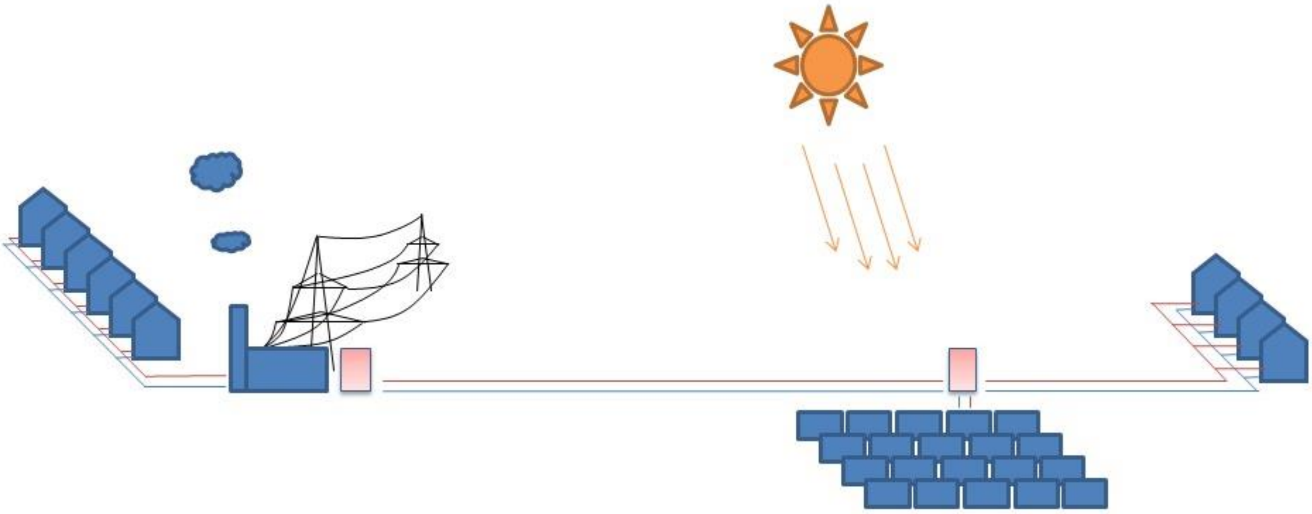

Integration of Solar Thermal Systems in Existing District Heating Systems

Master's Thesis in the Master's Programme Sustainable Energy Systems

CARLO WINTERSCHEID

Department of Civil and Environmental Engineering
Division of Building Services Engineering
CHALMERS UNIVERSITY OF TECHNOLOGY
Master's Thesis BOMX02-16-84
Gothenburg, Sweden 2016

MASTER’S THESIS BOMX02-16-84

Integration of Solar Thermal Systems in Existing District Heating Systems

Master’s Thesis in the Master’s Programme *Sustainable Energy Systems*

CARLO WINTERSCHEID

SUPERVISORS:
Prof. Jan-Olof Dalenbäck
Prof. Stefan Holler (HAWK University of Applied Sciences and Arts Hildesheim/ Holzminden/ Goettingen, Germany)

EXAMINER:
Prof. Jan-Olof Dalenbäck

Department of Civil and Environmental Engineering
Division of Building Services Engineering
CHALMERS UNIVERSITY OF TECHNOLOGY
MASTER’S Thesis BOMX02-16-84
Gothenburg, Sweden 2016

Integration of Solar Thermal Systems in Existing District Heating Systems
Master's Thesis in the Master's Programme Sustainable Energy Systems
CARLO WINTERSCHEID

Examensarbete BOMX02-16-84/ Institutionen för bygg- och miljöteknik, Chalmers tekniska högskola 2016

Department of Civil and Environmental Engineering
Division of Building Services Engineering
Chalmers University of Technology
SE-412 96 Göteborg
Sweden
Telephone: + 46 (0)31-772 1000
CHALMERS UNIVERSITY OF TECHNOLOGY
Master's Thesis BOMX02-16-84
Gothenburg, Sweden 2016

Department of Civil and Environmental Engineering, Göteborg, Sweden, 2016

Integration of Solar Thermal Systems in Existing District Heating Systems

Master's thesis in the Master's Programme Sustainable Energy Systems

CARLO WINTERSCHEID
Department of Civil and Environmental Engineering
Division of Building Services Engineering
Chalmers University of Technology
CHALMERS UNIVERSITY OF TECHNOLOGY
Master's Thesis BOMX02-16-84
Gothenburg, Sweden 2016

ABSTRACT

Modern district heating networks are usually operated with a changing flow temperature to cover the heat load of the supply area, depending on the outside temperature. Due to the minimum temperature requirements of individual customers, district heating (DH) networks also need to operate during the summer months. During this time, the load on the system is relatively low. This requires combustion facilities to also operate on low load levels. These systems have a potential of improving the energy efficiency by utilizing other energy sources such as waste heat from industrial processes or solar thermal systems. The overall aim of the presented work is to provide a methodology for the integration of solar heat into district heating

The feasibility to include solar thermal systems in existing DH networks will be analysed based on the state-of-the-art of solar district heating (SDH). The main focus will be on large DH systems that are mainly supplied by fossil combined heat and power (CHP) plants considering how such plants can be operated in the future. Results will display characteristic technical, economic and ecological key performance indicators of the transformed DH system.

Key words: district heating, solar district heating, solar thermal systems

Contents

Preface

In this study, numerous calculations have been performed to analyse and evaluate various solutions of integrating a solar thermal system in an existing district heating system. The calculations have been carried out from February 2016 to May 2016. This project work is part of a research project the HAWK University of Applied Science and Art Göttingen, Germany has together with a utility company in southern Germany under the guidance of Professor Stefan Holler. As the development of the project in the future is uncertain the utility company prefers not to be named in this report.

This project work has been carried out under the guidance of Professor Stefan Holler in Germany and Professor Jan-Olof Dalenbäck in Sweden. Research and calculations were performed in the offices of the Department of Resource Management, HAWK University of Applied Science and Arts Göttingen, Germany and supported with data sets from the utility company.

Finally, I want to thank the following people for the support during the process of this thesis:

Profesor Jan-Olof Dalenbäck who supervised and examined my work in Gothenburg but also in phone calls while I was in Germany.

Professor Stefan Holler who supervised me in Göttingen and supported me to get contacts and necessary information.

Professor Ulrike Jordan who enabled me to take part in a PhD course on "Applications of Large Solar Heating Systems" at the University of Kassel.

The PhD students of the "Solar Heat Integration Network" (SHINE) for technical as well as moral support.

Göttingen, August 2016

Carlo Winterscheid

Notations

Roman upper case letters

A	aperture area needed	[m²]
c	heat capacity of water	[Wh/(kgK)]
G	global radiation	[W/m²]
$\dot{Q}_{sol,dir}$	directly used solar heat rate	[MW]
$\dot{Q}_{dis}$	storage heat discharge rate	[MW]
$\dot{Q}_{sol,stor}$	stored solar heat rate	[MW]
$\dot{Q}_{add}$	additional heat supply rate	[MW]
$\dot{Q}_{dem}$	heat load of the sub-network	[MW]
Q_{ch}	level of storage charge	[MWh]
$Q_{dem,m}$	monthly energy demand by the sub-network	[kWh]
Q_{re}	daily storage heat energy recharge	[MWh]
Q_{st}	storage energy capacity	[MWh]
$Q_{sol,m}$	monthly energy to be supplied by solar	[kWh]
$Q_{dem,tot}$	annual energy demand by the sub-network	[kWh]
Q_{sz}	annual energy chosen to be supplied by solar	[kWh]
Rel	relative monthly energy demand	[-]
T_{max}	maximum storage temperature	[°C]
T_{min}	minimum storage temperature	[°C]
T_{in}	hourly collector inlet temperature	[°C]
T_a	hourly ambient temperature	[°C]
T_m	hourly medium temperature	[K]
T_{out}	hourly collector outlet temperature	[°C]
V	storage volume	[m³]
ϱ	density of water	[kg/m³]

Roman lower case letters

$\eta 0$	collector zero-loss efficiency	[-]
$a1$	first degree coefficients of the collector heat losses	[W/Km²]
$a2$	second degree coefficients of the collector heat losses	[W/Km²]
$q_{sol,m}$	specific net solar gain per month	[kWh/m²]

Abbreviations

CHP	combined heat and power
DH	district heating
ETC	evacuated tube collector
FPC	flat plate collector
PEF	primary energy factor
SDH	solar district heating

1 Introduction

The general idea behind including solar collector fields in DH networks is to lower or even completely supply the low heat demand of a DH network during the summer months. Since the 1980s Denmark and Sweden have built many solar heating plants (Fisch et al. 1998). In some of these cases a seasonal storage is used to provide a solar share even above 50 % of the total system demand. The high taxation of primary energy sources supported these ambitions in Denmark, that lead to seasonal storages which are only feasible on a very large scale (Meißner et al. 2012). In comparison to the Danish and Swedish developments SDH systems in Germany started to be built later, at the beginning of the 1990s. Even though the number of large solar heating plants especially in Europe is rising, the international implementation of SDH systems is not yet very widely spread (Frederiksen & Werner 2013).

The large DH systems in Germany are usually supplied by large CHP plants. These plants are often operating as base load power producers and can supply heat and electricity at a cost-efficient level during summer and winter, also due to funding by the CHP production law (Kraft-Wärme-Kraftwerk-Gesetz KWKG) (Berberich et al. 2015).

In addition to the availability of low-cost heat, high and very high system temperatures in the DH systems also prevented solar heat generating systems (Urbaneck et al. 2015). In the case of the DH system Chemnitz, only a large change in the system structure in one district made a change feasible. Possibilities of including solar collector systems in existing DH networks that are not about to change radically and are using large scale CHP plants as a main heat source were rarely analysed.

From 2013 to 2015 the German solar thermal research institute Solites conducted a study on combining CHP systems with large solar heating plants (Berberich et al. 2015). This study highlights the development towards more fluctuating electricity prices which already has large impact on some CHP plants. The annual full load hours of German CHP plants will decrease in the future if the plants are operated according to the electricity price, which is expected to decrease. This reduction in operating time during the summer months, when solar PV penetrates the electricity market more strongly, also opens the possibility to implement solar thermal systems. Such a situation can open the possibility to shut down CHP plants at hours when it would be unfeasible to operate them according to the electricity price.

The Solar-KWK report by Solites already provides a good background to the given system. In contrast to the Solar-KWK report this project focuses on a specific existing system and analysis the option of supplying a sub-network with solar heat during the summer season. Special in this case is also that the sub-network needs to operate with higher supply temperatures than the main-network.

Commonly when integrating SDH into DH networks, parts with lower temperatures are operated with solar thermal support, as it is the case in Chemnitz, Germany. In the given case it is vice-versa due to the large CHP plant in the main-network.

This work elaborates aspects of how a solar collector field can be beneficial for a DH system based on a large scale CHP plant and how such a collector field can be included. The work was carried out by evaluating the load pattern of a part of an existing DH system in Germany and designing possible system solutions. In the given case the system analysis was based on the following conditions:

- a fixed supply temperature in a connected sub-network that is not needed in the whole system
- a long connection pipeline between the main network plant and the connected sub-network
- a reduction of the primary energy factor (PEF)
- a reduction in CO_2 emissions

Taking into account the interests of the network owner different methodologies of including a solar collector field were developed. In the given case a solution without a local backup boiler is preferred; instead a daily reheat of a storage from the large CHP plant was suggested.

Figure 1.1 underlines the focus of this project on the interaction between the two network parts and a possible SDH plant. Details of the CHP plant, the main-network or the sub-network are not analysed in this project.

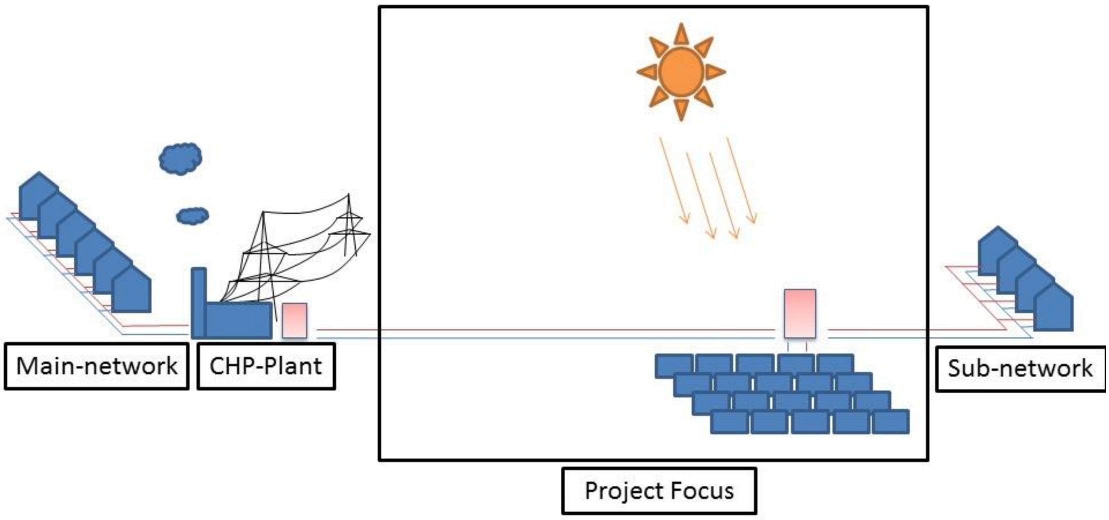

Figure 1.1: Project focus: The solar thermal field and the thermal storage are located between main-network and sub-network

2 Background

This background chapter gives general information about the different topics the project works with.

2.1 District Heating

The term district heating stands for an energy service, mostly provided in areas with a higher population density. District heating systems have locally supplied thermal energy and a local thermal energy demand. The system then connects supply and demand with a piping network to distribute the hot water. The hot water can be used for space heating but also for domestic hot water production. In some cases, it is also used for industrial processes.

The energy sources for DH systems can be CHP plants, waste-to-energy plants, industrial waste heat or plants that can deal with difficult e.g. bulky primary energy sources that a domestic boiler can't deal with. In some cases, large heat-pumps, electrical boilers or solar thermal systems are also used in DH systems. This project deals with the possibility of using CHP plants in combination with solar thermal systems.

To operate a DH network economically it is necessary to have cheap thermal energy to balance investment and maintenance costs for the piping network (Frederiksen & Werner 2013).

The example used in this project is located in Germany. In Germany about 13 % of all dwellings were connected to a DH network in 2010. With 32 % connected dwellings in the eastern federal states and 9 % connected dwellings in the western federal states the share of connections in eastern Germany is substantially higher.

About 83 % of the DH systems in Germany are supplied with thermal energy from a CHP plant. These plants are normally supplied by coal, natural gas or lignite. The share of renewable energy in German DH systems is about 9 % and is based on waste incineration (7 %) and Biomass (2 %) – solar thermal energy does not exist at a mentionable rate in German DH systems but is discussed in some scenarios to increase in importance (AGFW 2013).

2.1.1 Solar District Heating

Domestic solar thermal heating systems are a mature technology to provide hot water at temperatures below 100 °C. So far solar thermal systems are mainly used for individual dwellings.

The large scale systems integrated in a district heating network are so called SDH plants. These can be centralized ground mounted collector fields with a thermal storage or distributed collectors that can be mounted on roofs and are connected to the DH network. It can also be differentiated between short term and seasonal storages. Short term storages can be tank storages that can have many intervals of charging and discharging due to their smaller size relative to the DH systems demand and do usually not provide more than 20 % solar fraction. In contrast seasonal storages store a surplus of heat during summer months, which normally have a low heat demand, compared to winter months with higher heat demand and lower solar gains. Figure 2.1 shows a design for a centralized SDH plant.

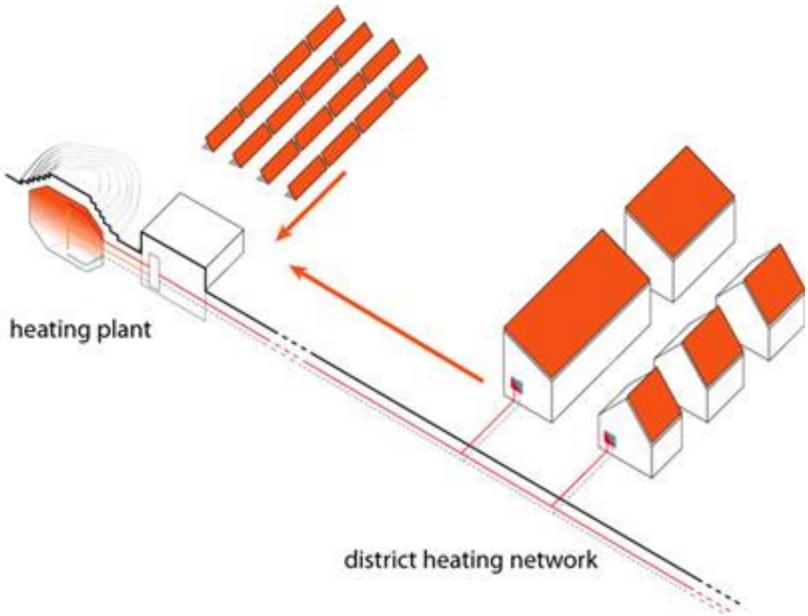

Figure 2.1 Centralized SDH plant from (Source: Solites)

2.1.2 Collector types

The most common collector types for SDH plants are flat plate collectors (FPC). evacuated tube collectors (ETC) are also used in some project but not yet to the same extend as FPC.

When building solar thermal energy systems, the maximum ambient temperatures and their influence on the collectors have to be considered. During winter low temperatures can lead to freezing of the heat transferring liquid in the pipes. Freezing can be avoided by adding glycol to the water in the collector field. This requires a heat exchanger to separate the glycol-water system from the thermal storage water and the DH network. Additionally, the net solar gains will be 3 % to 5 % lower because the values for the collector efficiency are measured with water as a heat transferring liquid. Furthermore, systems with a glycol-water mixture need to have larger pipe dimensions to have the same pressure drop compared to water based systems due to the lower viscosity. During summer, low heat demand can lead to stagnation and evaporation in the collector pipes. To avoid this, thermal storages are often over dimensioned or cooling systems for the collector field are installed. Some existing ETC systems operate only with water in the collectors. In these cases, about 1 % to 4 % of the provided annual solar thermal energy are needed for active frost protection. (Meißner 2016)

2.1.3 Existing systems

In Europe there are currently 163 plants with more than 700 kW_{th} and 82 SDH plants with more than 1 MW_{th}. Denmark has the most installed systems in a country comparison. Most large systems use FPC to supply the heat do district heating systems. A few systems that have a large collector area also use seasonal thermal energy storages. As of now, spring 2016, only 16 SDH plants are listed with an aperture area above 15 000 m² collector aperture area. Systems that utilize a centrally existing CHP plant for a storage recharging process as it is analysed in this work are not known. (Solites 2015)

2.2 Primary energy factor

The primary energy factor PEF is in Germany calculated according to the AGFW worksheet FW 309 part 1.

The PEF covers all demands and losses that appear within the fuel refinery, energy production, energy storage and energy distribution

Depending on the energy source in a DH system different factors are used on the provided energy. If the provided energy is based on industrial waste heat or renewable energy sources this factor is for example zero. (AGFW 2010)

2.3 Funding in Germany

In this part of the background some market influencing policy measures in Germany are briefly explained.

2.3.1 Applicable funding for large solar heating systems

In Germany the ministry of economy and energy (BMWi) offers support schemes which coordinated in the KfW-program:

- Solar heating systems of 40 m² or more that supply heat mostly to a heating network can receive a dept retirement of 40 % of the investment costs at a maximum of 10 Mil. €.
- District heating networks can receive a dept retirement of 60 €/m pipeline length of the investment costs at a maximum of 1 Mil. €. Additionally, domestic substations can be funded with 1800 €.
- Thermal energy storages larger than 10 m³ can receive a dept retirement of 250 €/m² if they are mainly supplied by renewable energy sources. The maximum that can be funded for thermal energy storages is 1 Mil. €.

(Pauschinger 2015)

2.3.2 Subsidies for energy from CHP plants

The KWKG (Kraft-Wärme-Kopplungs-Gesetz) is the law to regulate operation and subsidies for German CHP plants. In the current version it allows funding for each kWh of electrical energy that is fed into the electricity grid. The funding depends on the CHP plant type as well as on the size of the plant. Larger plants receive less funding. Additional funding can be received from the Federal Office for Economic Affairs and Export Control (BAFA) for the district heating network construction or extension. As it is possible for SDH thermal energy storages also CHP plants can receive 250 €/m³ funding for thermal energy storages, but its maximum is set to 5 Mil. €. (BDEW 2013)

2.3.3 Influence of the PEF on building construction projects

The ENEV (Energie-Einspar-Verordnung) is an energy saving law that regulates the annual primary energy consumption of newly constructed buildings. This is done by regulating insulation standards and technical equipment. If a building is connected to a district heating network the primary energy factor of the district heating network is taken into account when the building is evaluated. A building that fulfils certain standards can receive additional funding. In order to meet the standards, the PEF of a DH network has to be low enough. In the coming years the ENEV will become stricter regarding the accepted primary energy consumptions of buildings. Even though CHP based DH networks have an advantage for the calculation of the PEF stricter requirements might require changes in the networks. If a PEF of a network is too high building owners that connect to the DH systems might have to install additional systems in order to have an overall lower PEF. (Lubinski 2014)

3 Methods

SDH projects require detailed planning to meet the demands of clients at all times. Compared to DH systems based on fossil fuels that can be stored without losses, SDH systems have the additional challenge to meet the intermittency of solar radiation. Solar radiation is not only varying depending on the local weather conditions but also depending on the geographical location of the planned SDH plant.

In this project an example site in southern Germany was chosen. Climate data and data of a sub-network of a DH network have been used to present the chosen calculation method. In this section the tools as well as the steps that lead to the results in Chapter 4 are explained in detail.

In the field of SDH a range of numerical tools are used. The tool that is mostly used in the reviewed literature is TRNSYS. Furthermore a range of freeware tools like F-easy, Fjernsol II, SDH online-calculator and Sunstore 4 are available and can be found on the SDH webpage (Solites 2015). A short explanation and description of tools for SDH can be found in Le Denn 2013.

In this study the calculations were performed in the numerical computing environment MATLAB using data of the sub-network and weather data from PVGIS (European Commission). Choosing MATLAB resulted in more detailed results compared to the freeware tools. It enables to import weather data from PVGIS for any chosen site in Europe and to graphically analyse the results in detail. Furthermore, it enables calculating thermal storage sizes depending on the given requirements. The software TRNSYS can also calculate demands as described and offers high flexibility. This flexibility requires a deep understanding of the calculation patterns that lay behind the modular structure. To avoid mistakes the user has to have certain expectancies of the results. As a number of detailed technical parameters needed for such a calculation were unknown and would depend on differing, often empirical values were chosen to perform a simplified calculation in MATLAB. The calculation was simplified by mainly calculating with energy flows and not with mass flows of a medium at a given temperature with a specific heat capacity. This decreases the risk of choosing inappropriate values for the mass flow, the heat capacity and the temperature levels.

At the beginning of the thesis project different approaches of the methodology were discussed. It quickly turned out that supplying the energy demand of the sub-network during the summer season only by solar heat would lead to an oversized collector field and storage. One main ambition was to reduce the dependency of the DH sub-network from the DH main-network during the summer season. To design a more competitive system, a back-up boiler as it exists in other SDH plants must be installed to meet peak demand hours or hours of low solar radiation with an empty thermal storage.

In case of a CHP based system, the thermal peak demand can also be covered by the CHP plant. A problem can be the requirement of quickly changing demands in the sub-network if the pipeline to the sub-network is long and contains water that has already cooled down. In such a case the water on the needed temperature level has to be pumped over the distance from the main-network to the sub-network. If the distance between the DH network parts is longer, this will cause a mentionable time delay. A solution to that problem can be to regularly recharge a thermal storage that is located close to the SDH plant and the sub-network. The developed methodology in this study is based on such a thermal storage that is placed closely to the solar collector field and the DH sub-network.

3.1 Calculation steps

Figure 3.1 below shows the input and output parameters as well as values that need to be calculated to receive the output parameters These output parameters are needed to analyse the benefits of a SDH plant.

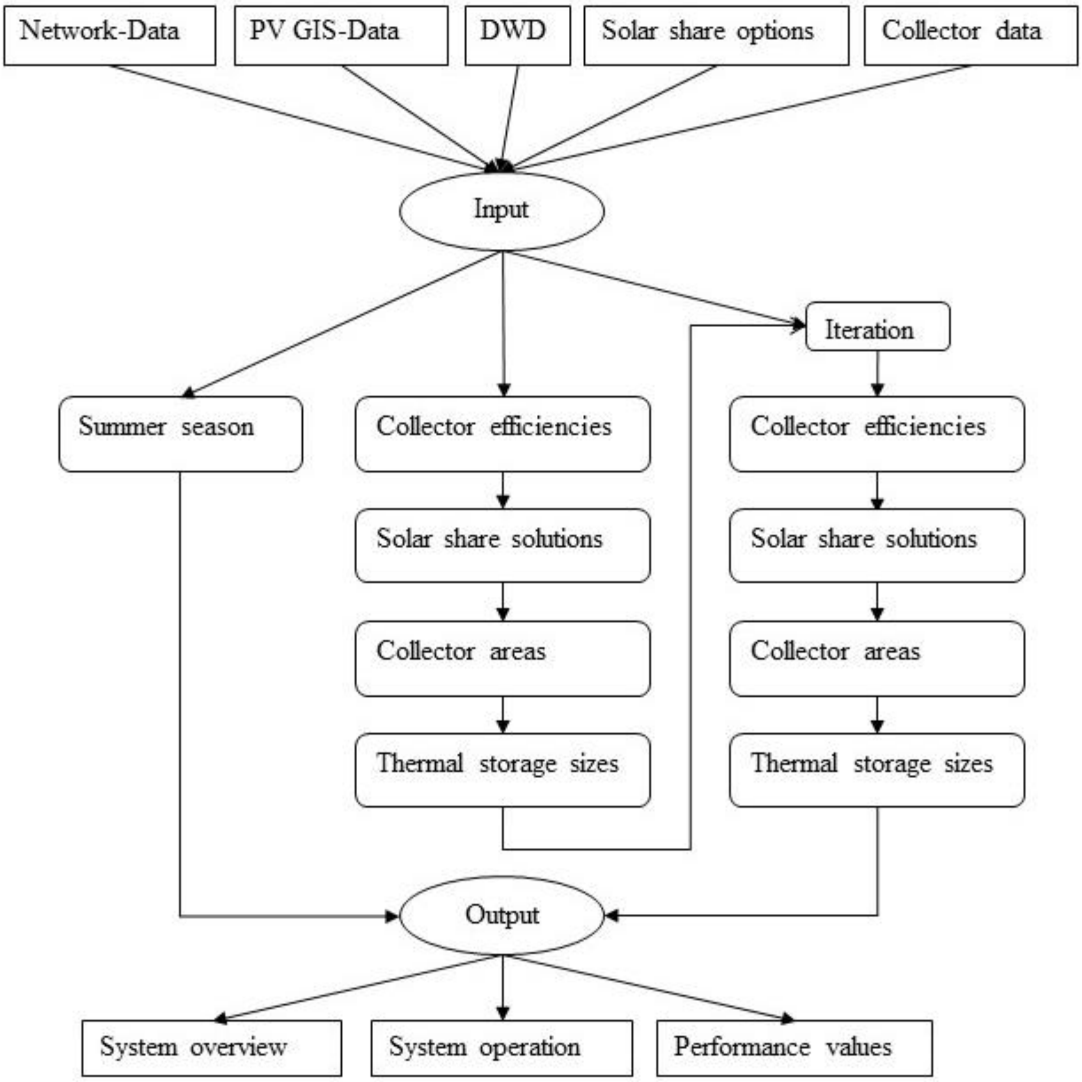

Figure 3.1 Methodology for the integration of solar heat into existing DH systems

3.1.1 Input

As Figure 3.1 shows the input parameters consist firstly of the available four years of hourly measurements of heat consumption, volume flow and flow temperatures of a sub-network. Secondly, values in 15 minute time steps for the solar radiation of an average day of each month were imported from PVGIS for the specific location. Thirdly weather evaluation has been performed using outdoor temperature data from 1974 to 2014 from Deutscher Wetter Dienst, DWD (Germany's National Meteorological Service). Furthermore, different solar fractions where chosen to be able to compare different scenarios as well as two different collector types: one flat plate collector and one evacuated tube collector.

Figure 3.2 and Figure 3.3 show the average load Q_{av} of 2013 to 2015 of the sub-network as well as the solar radiation G on a 1 m² surface oriented south with an angle of 35 ° as it was imported into the calculation from PVGIS. The orientation south with an angle of 35 ° offers the largest solar gain throughout a year. In PVGIS the radiation is given in 15 minute steps for an average day of each month. Accordingly, to display the 8760 h of one year the representing days of each month had to be put in series as often as each month has days. Therefore, Figure 3.3 contains 365 curves of solar radiation for each day with 12 different amplitudes depending on the month.

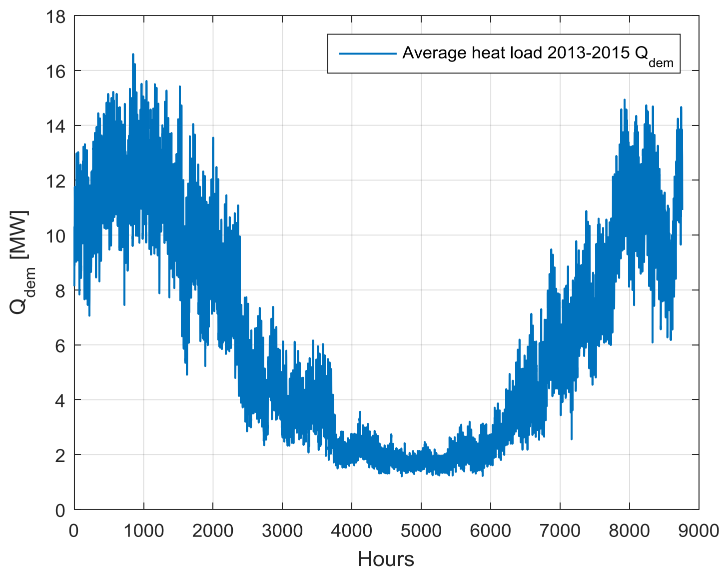

Figure 3.2 Example of annual the heat load curve in a sub-network

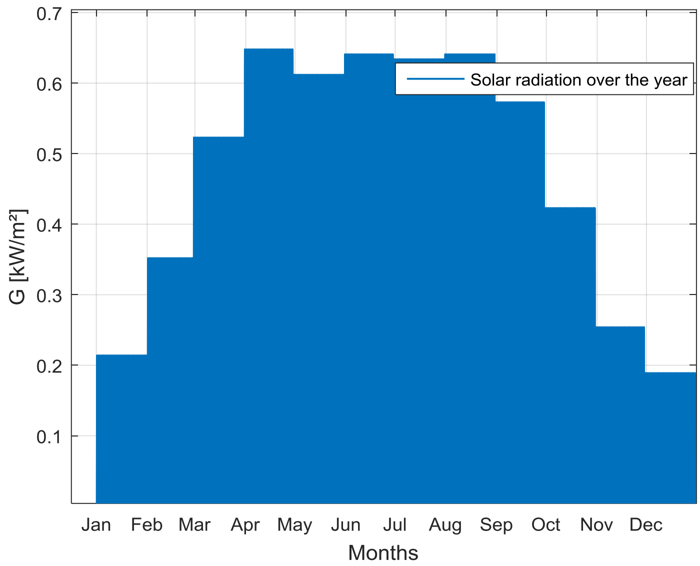

Figure 3.3: Example of maximum solar radiation on an average day on a south oriented 35 ° tilted surface in southern Germany

3.1.2 The summer season

A summer season needs to be defined to be able to compare in how far a thermal solar collector system is able to supply the sub-network with energy independently from the main-network. As explained in the introduction it is one goal to be able to operate the main-network during the summer season independently from the sub-network.

For this part of the calculation the weather data from the Deutscher Wetter Dienst, DWD (German meteorological service) and a heating curve that visualizes the DH supply temperature of the sub-network at a certain outdoor temperature were used. With the data supplied by DWD the average outdoor temperature of an example year based on temperature measurements from 1974 to 2014 was calculated. Together with a function based on the heating curve, an expected DH supply temperature was calculated. This temperature has been smoothened and is shown as a pink dotted line in Figure 3.4 together with the average DH supply and return temperature of the sub-network for each day based on the years 2013 to 2015. The summer season is defined by the first and last day when the expected DH supply temperature is 75 °C. The supply temperature is limited by the heating curve which requires 75 °C even at higher ambient temperatures. The summer season that is marked with two black lines in Figure 3.4 starts on the 16th of May and lasts till the 22nd of September.

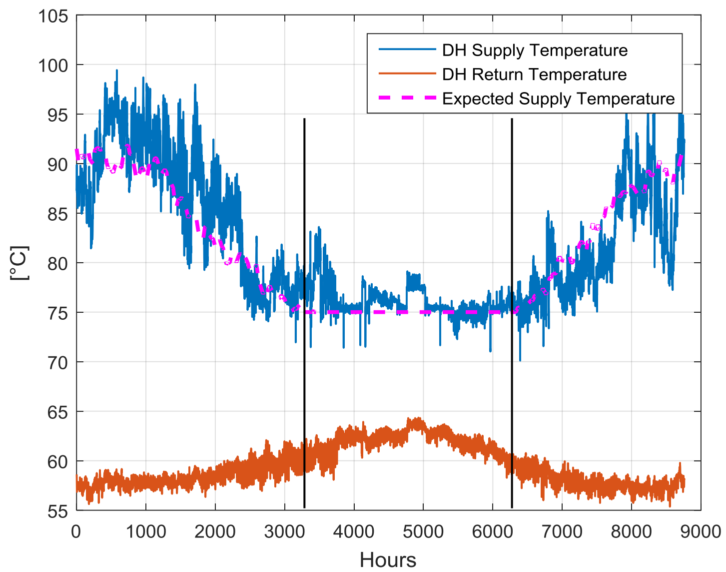

Figure 3.4: Average supply and return temperature and expected supply temperature of the sub-network

During the summer season it is expected that the DH main-network can lower its supply temperature if it can operate independently from the sub-network, whereas the sub-network needs to keep 75 °C as a minimum temperature.

3.1.3 Collector efficiencies

With the calculation of the collector efficiencies η_c the main calculation line visualized as the central part in Figure 3.1 is entered. For this calculation sub-network data, PVGIS data and collector data are used.

The efficiency calculation of solar thermal collectors η_c is explained in the European Standard EN 12975 (Kovacs 2012). This calculation method was also used in this study and bases on the following equations:

$$\eta_c(t) = \eta_0 - a_1 \frac{(T_m(t) - T_a(t))}{G(t)} - a_2 \frac{(T_m(t) - T_a(t))^2}{G(t)} \tag{1.1}$$

$$T_m(t) = \frac{(T_{out}(t) + T_{in}(t))}{2} \tag{1.2}$$

Accordingly, the net solar gain $Q_{sol}(t)$ is:

$$Q_{sol}(t) = \eta_c(t) * G(t) \tag{1.3}$$

The average global irradiance $G(t)$ from PVGIS is given in 15 minute steps and was reduced to hourly steps in order to use the DH return temperature as collector inlet temperature T_{in} and the DH supply temperature as the collector outlet temperature T_{out} if it was above 80 °C, otherwise T_{out} was set to 80 °C. The minimum temperature of 80 °C allows temperature losses over the pipes as well as through heat exchangers so that a supply temperature in the DH sub-network of 75 °C can still be met. The ambient temperature T_a was taken from PVGIS as well. The collector dependent values η_0, a_1 and a_2 were taken from the manufacturer's data sheets of a representative flat plate collector (FPC) and a representative evacuated tube collector (ETC). The data sheets are attached in Appendix B.

The collector efficiency was calculated for every hour of an example year and is visible in Figure 3.5 below. Due to the slope of 35 ° the maximum daily efficiency during the summer months is rather constant. During the winter months' flat plate collectors generally perform worse due to the lower radiation and the sensibility to low ambient temperatures.

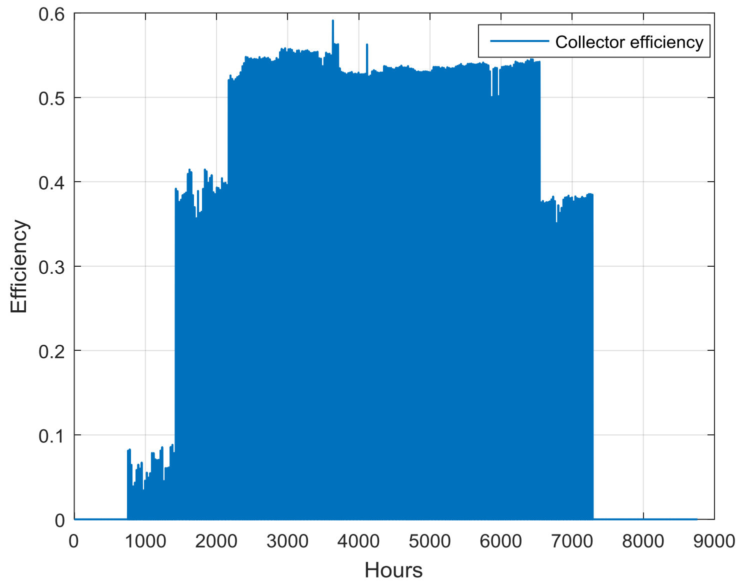

Figure 3.5: Hourly collector operation point efficiency for an example year

3.1.4 Area selection:

The required collector areas were calculated depending on different annual solar shares of 5, 10, 15, and 20 % of the total annual heat consumption. Additionally, one approach aims to supply the heat consumption of July completely, which corresponds to about 14 % solar share in case of a good flat plate collector. July has been chosen because this is the month with the lowest heat demand throughout the year. The following calculation steps are used to receive the actual collector aperture area in m²:

$$Rel(t) = \frac{Q_{dem,m}(t)}{Q_{dem,tot}} \tag{1.4}$$

$$Q_{sol,m}(t) = Q_{sz} * Rel(t) \tag{1.5}$$

$$A = \max\left(\frac{Q_{sol,m}(t)}{q_{sol,m}(t)}\right) \tag{1.6}$$

With equation (1.4) the relative heat supply of each month $Rel(t)$ can be calculated. The sum of all $Rel(t)$ values for each month is 1. It is based on the monthly energy consumption $Q_{dem,m}(t)$ [kWh/m²] divided by the annual heat supply $Q_{dem,tot}$ [kWh/m²]. In equation (1.5) the monthly supplied energy $Q_{sol,m}(t)$ [kWh/m²] was calculated depending on the total energy amount of a chosen scenario Q_{sz} and the factor $Rel(t)$ for each month. Q_{sz} is 5, 10, 15, or 20 % of $Q_{dem,tot}$ or the total energy consumption of July. The last equation for the area calculation, equation (1.6), calculates the maximum aperture size A [m²] that would be needed during each month to supply the required energy. For each month it divides the monthly needed total solar gain $Q_{sol,m}(t)$ [kWh] by the specific solar gain per m² that can be supplied in each month $q_{sol,m}$ [kWh/m²]. The calculated area is the aperture area, which is the collector area without the collector frame. For the field size it is necessary to calculate a row distance and the distance between each collector. In this project the distance between each collector was set to assumed 20 cm. The row distance calculation is based on the location because shading of the collectors has to be avoided. The flat plate collectors chosen for the study hardly supply any heat from November to February. Accordingly, shading within the collector rows within those months can be accepted. The evacuated tube collectors supply heat during the winter months and should therefore have a larger row distance. The sun angle at which the collectors shall not shade each other was set to 25 ° and 17 ° for the flat plate collectors and the evacuated tube collectors respectively. To calculate the collector field size, the aperture area was multiplied by a factor. This factor comprises the collector dimensions, the distance to the next collector and the lowest accepted sun angle. For a flat plate collector, the calculated factor is 2.27, for the evacuated tube collector the factor is 3.20. This factor needs to be multiplied with the aperture area to get the total collector field area. Figure 3.6 shows an overview of different solar shares and the resulting monthly solar energy production. Besides the monthly solar gain and the monthly sub-network demand is shown. At this stage of the calculation it is expected that all solar surplus during the summer months of the larger solar share scenarios can be stored.

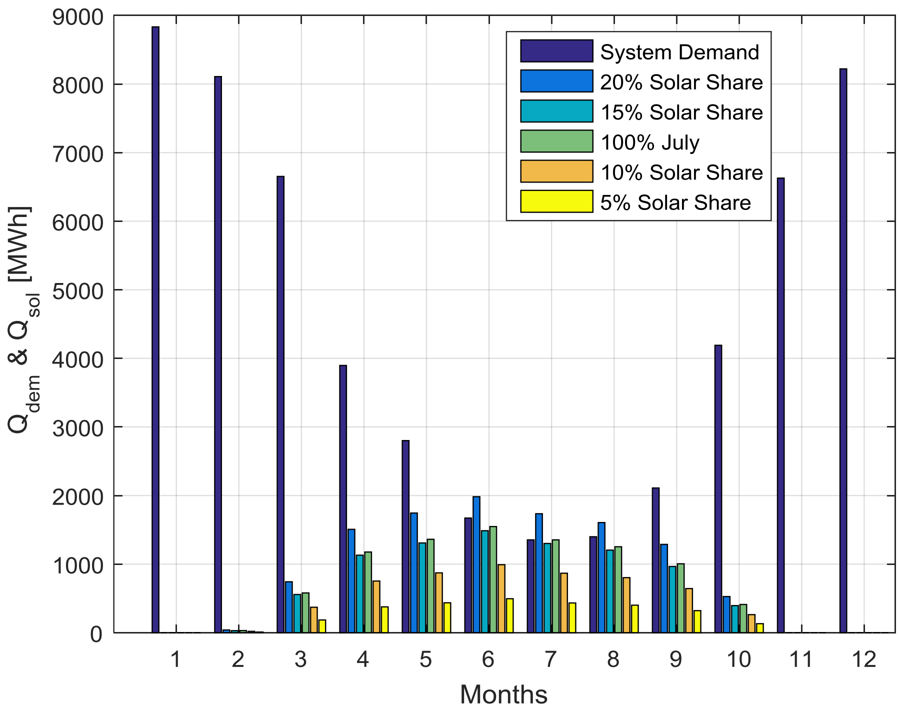

Figure 3.6: Net solar gain compared to demand for different solar share variations

Table 3.1 presents an overview of the calculated variations of the collector and field area as well as the specific and absolute thermal storage volume.

Table 3.1: Calculation results for different annual solar share

Solar share [%]	Actual solar share [%]	Collector area [m²]	Field size [m²]
5	5	6,507	13,791
10	10	13,029	27,581
100 % July	14	18,319	38,808
15	14.8	19,536	41,372
20	17.8	26,044	55,163

3.1.5 Storage Dimensioning

In the tools SDH Online-Calculator and Sunstore-4 values of 50 to 300 l of water per m² collector area are recommended or allowed as the specific storage volume for short term thermal storages. In contrast to those values, other literature as Meißner et al. (2012) points out that SDH thermal storages are often dimensioned larger than needed.

For this project it was required to store only the surplus solar heat that can be received within a single day and to dimension the storage size accordingly. The thermal storage size was dimensioned by the following equation:

$$Q_{st}(t) = \sum(|\int_t^{t+24} Q_{Sol} - \int_t^{t+24} Q_{dem}|) \tag{1.7}$$

Figure 3.7 shows the solar surplus of each day that can be received using an average annual load curve of the example system and a solar collector field size corresponding to the July demand (annual solar share 14 %).

The conversion from MWh storage capacity to m³ water in storage capacity was performed according to the following equation:

$$V = \frac{Q_{st}}{\varrho * c * (T_{max} - T_{min})} \tag{1.8}$$

T_{min} is the DH return temperature that has a measured maximum of 63 °C. T_{max} is the maximum allowed temperature in the storage, in the considered case 95 °C (Meißner 2016). ϱ, the density of water, was set to 971,8 kg/m³, while c the heat capacity of wather is 1,166 Wh/kgK. Both values are constant in equation (1.8).

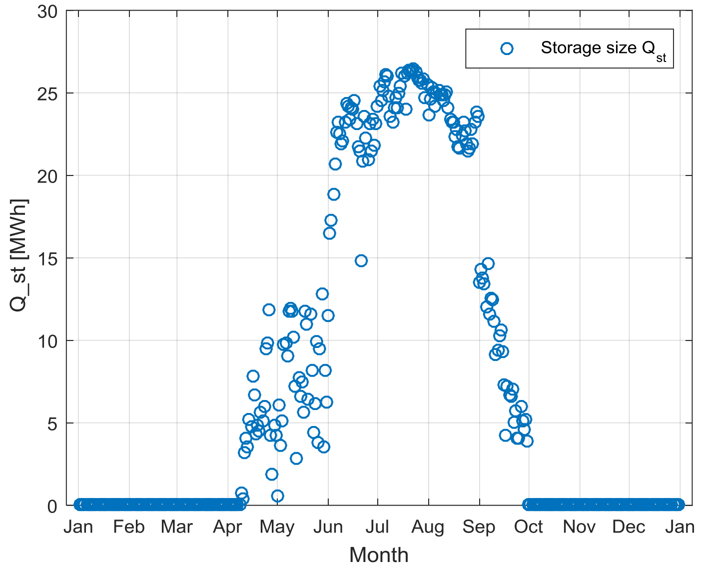

Figure 3.7: Needed storage capacity to store the solar surplus energy for an annual solar share of 14 %

3.1.6 Storage operation

To enable the sub-network to operate as independently as possible without having a backup boiler it is considered that the storage is reheated once per day. In this scenario the recharge from the main-network is set to be done every evening at 9 pm with a supply temperature of 80 °C. This means that during summer time three different temperature zones will develop in the storage: one with the DH return temperature, one with 80 °C from the CHP plant and one with a maximum of 95 °C from the collector field.

3.1.7 Iteration

With the iteration, the right branch of Figure 3.1 is entered. Iteration is needed because the first calculation of the collector efficiency is based on collector outlet temperatures of 80 °C or higher in the winter months, but it was decided to operate the heat storage on a temperature level up to 95 °C. Therefore, the collector outlet temperature has to be increased for the time that the storage needs to have temperatures above 80 °C to store the calculated heat surplus.

In this study the collector outlet temperature for the collector efficiency calculation was set to:

1) 87.5 °C for the days that the storage has to have a heat capacity between 50 % and 75 % of its maximum capacity
2) 95 °C for days the storage has to have a heat capacity of 75 % to 100 % of its maximum capacity

As a result of that iteration all steps of the past calculation have to be repeated with the new calculated efficiency values. The required collector area and storage size increase to be able to provide the same amount of energy for the solar share that is to be calculated. In the case of the scenario that shall supply energy equal to the demand in July, the annual solar share increases as well because in this case the calculation starts with the energy amount that needs to be supplied during a single month and not during the whole year.

3.1.8 Additional performance indicators

Based on the already calculated values additional technical, ecological and economical parameters were calculated. With these values different scenarios can be compared better and a comparison to other planned and existing plants is possible.

The technical parameters for comparison are the annually received solar radiation, the net solar energy gains, the specific annual net solar energy and the losses of solar energy that occur because the storage is for some time during the summer season loaded to its maximum and cannot receive more solar heat.

The ecological parameters for comparison are the CO_2 emissions that are avoided due to the supply of solar thermal energy instead of CHP energy. In the calculation of the reduced CO_2 emissions a value of 178 g CO_2/kWh heat was used for thermal energy that is received from the CHP plant. Furthermore, the PEF was calculated to visualize how far a scenario can help to meet future requirements in PEF reduction to get a financial support for house owners (Chapter 0). The PEF was calculated based on a given PEF of the main-network and the additional solar heat that has a factor of 0 if electricity consumption of pumps etc. in the solar plant is neglected. The reduced PEF can then be used to calculate a new PEF of the sub-network that also takes into account the DH losses of the sub-network. The modified PEF was calculated using the following equation:

$$PEF_{mod} = \frac{(Q_{CHP} * PEF_{main} + Q_{sol} * PEF_{sol})}{Q_{tot}} \tag{1.9}$$

The economical parameters are based on the thermal storage size and collector area as well as discounting factors like discounting time and interest rate. Additional expenses are represented by a factor as it is done by the SDH Online-Calculator and (Pauschinger 2015). The listed percentages can be found in Chapter 4.2.

For the specific thermal storage price, the specific collector price and the specific land price fixed values were used. Therefore, the economy of scale is not visible in the financial evaluation. The economical key parameters will be the total investment costs in €, the annual costs in €/a, the specific price of heat in €/MWh and the specific CO_2 reduction costs in €/tCO_2.

3.2 Validation methods

The used method for calculation is more detailed compared to some freeware tools which are mentioned in the beginning of this Chapter, but does not consider the same amount of physical background calculations most of the professional tools offer. This difference in the method makes it hard to compare results directly to results from other methods. To verify that the results are in a general realistic range the SDH-online calculator was used. It bases on meteorological data from Meteonorm and a range of calculations were performed with TRNSYS that can be called up with the online form.

The SDH-Online Calculator allows choosing between a decentralized system without thermal storage and a centralized system with thermal storage. In both cases a big difference in solar radiation on the collector field was realized. This difference can be explained on the one hand by the different sources of solar radiation values, PVGIS and Meteonorm and on the other hand by the online calculator which allows to choose from 6 European locations – the location of the example case project in this study was not available and the closest different location was chosen for comparison.

Annual solar radiation on a collector field for the same location calculated by the online tool was about 9 % lower than solar radiation results by PVGIS for the same area, azimuth and collector slope. Due to the different location additional 5 % higher solar radiation was provided by PVGIS in comparison to the SDH-Online Calculator.

The decentralized calculation option is for systems that can directly supply the heat to the DH network and are relatively small dimensioned compared to the demand of the DH network.

The centralized calculation option includes an additional thermal storage to store a surplus of energy from the solar collector field. The smallest possible specific thermal storage dimension is 50 $l/m^2_{\text{collector field}}$, which is bigger than the results calculated to be necessary in this study.

In addition to the solar radiation values and the specific thermal storage volume, the exact solar collector values and the system temperatures differ in both calculations.

These large differences in the input values only allow a general comparison of the results. In order to give information about the expectable results a sensitivity analysis was performed. The results of the sensitivity analysis can be seen in Chapter 4.2.

4 Results and analysis

In the previous Chapter the method used for dimensioning different solutions for a solar collector field and a thermal storage was explained. In this Chapter the general output parameters and findings of the dimensioning process will be expressed in more detail. Furthermore, the results of a solar collector system with thermal storage in a DH system based on large scale CHP will be presented. To illustrate the results, the scenario of a solar collector field with a size that can supply the energy demand of the month July was chosen. It was decided to choose this scenario which equals about 14 % solar share, because on the one hand it offers a rather long time during summer where the sub-network can operate without additional heat supply and on the other hand it has only small losses based on a solar surplus that cannot be stored when the storage is fully charged.

4.1 Component size and operation

4.1.1 Collector field size

Using the method for calculating the collector field explained in Chapter 3.1.4, a certain area can be calculated for an ETC and a FPC that is able to supply an equivalent amount of energy as is consumed during July. Shown in Figure 4.1, the reader can compare the different solar energy supplied to the network during each month by each collector type. The collector field size in this example is dimensioned to meet the energy demand of July. To achieve this, the FPC needs to have a collector area 24 % larger than the ETC. When comparing the monthly system gains by solar energy of the two collector types, it is obvious that the FPC supplies hardly any energy during the winter months, even though the collector area is larger. This can mainly be explained by the higher thermal insulation an evacuated tube collector has. To supply the same energy amount in July both collector types need a different field size. The ETC has also got a larger system share in this example compared to the FPC as it is able to supply more energy during the winter months.

When scaling up both systems the same degree, losses in both systems would increase drastically during the summer months, as the systems do not operate with a seasonal thermal storage. The specific losses of the FPC would increase much faster compared to the ETC because the FPC supplies more of the annual energy production during summer compared to the ETC.

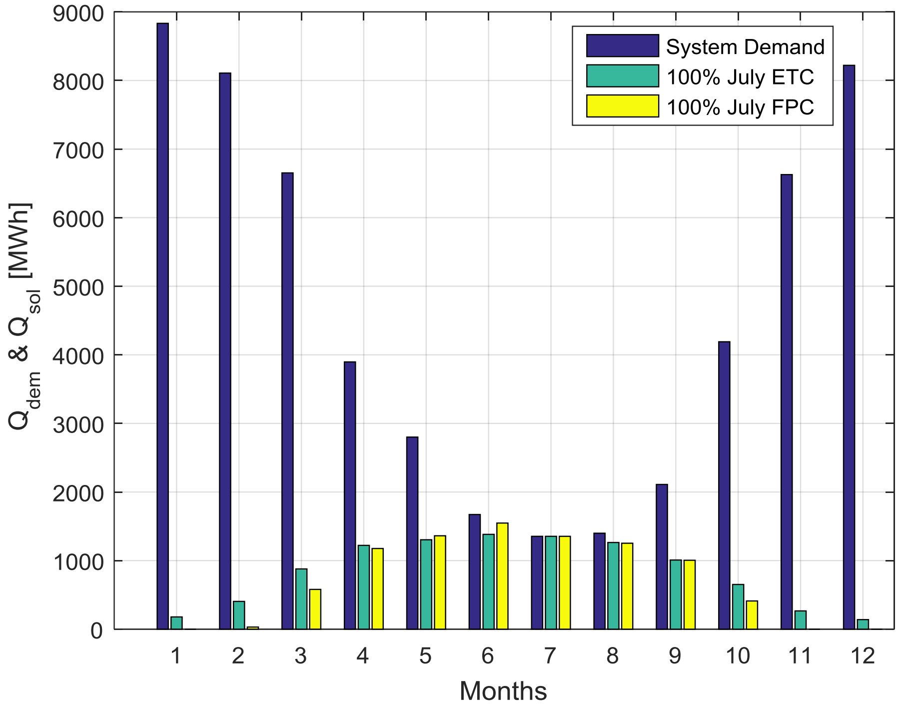

Figure 4.1: Monthly comparison of a ETC and a FPC in contrast to the monthly demand

4.1.2 Storage size

The next step of the calculation methodology after dimensioning the collector field size was the storage dimensioning. The calculation for the storage dimension resulted in specific thermal storage sizes to store a solar surplus. The specific thermal storage size of the calculated 100 % July FPC scenario was at 40 l/m² far below 50 $l/m^2_{collector\ area}$. Even in the 20 % solar share scenario the specific thermal storage size was 46 l/m². Specific thermal storage dimensions below 50 l/m² collector area were not found as recommended for short term thermal storages. In the case of some reviewed freeware tools it was even impossible to choose a size smaller than 50 l/m². For the SDH Online-Calculator used to compare values in Chapter 3.2 this can partly be explained because of the two system options: centralized and decentralized. A centralized system which includes a thermal storage has a rather large solar thermal system compared to the DH demand. Therefore, the solar surplus during the summer months would be larger and a bigger storage makes sense. In contrast to the minimum specific thermal storage sizes Meißner et al. (2012) recommend relatively small dimensioned thermal storages. Meißner et al. (2012) also point out that a solar storage normally is not used for the largest part of the year which underlines the economic importance to avoid oversized thermal storages. A similar experience was made in the presented work. If a solar thermal storage is not used as a power-to-heat thermal storage during the winter months, it is unused for about half the year as can be seen in Figure 3.7.

4.1.3 Operation

With the collector area, the thermal storage size and hourly temperature and radiation input, hourly system operation can be simulated. The simulation of this project is focused on the summer season when the aim is to operate the DH sub-network as independently as possible from the main-network.

Figure 4.2 and Figure 4.3 illustrate the supply and demand curves for the summer season as well as the state of charge of the thermal storage. The graphs are again based on a FPC system that is dimensioned to meet the July demand completely. The graphs in Figure 4.2 on the left side represent a system without a regular recharge of the thermal storage. The graphs in Figure 4.3 on the right side represent a system with a thermal storage recharge every evening at 9 pm.

The Figure 4.2a and Figure 4.3a show for both scenarios, without recharge and with thermal storage recharge, a demand $\dot{Q}_{dem}$ line in blue, a line for the directly used solar thermal input $\dot{Q}_{sol,dir}$ in red, a negative line for the solar thermal surplus that is stored in the thermal storage $\dot{Q}_{sol,stor}$ in yellow and finally a purple line that shows the energy that is taken from the storage to supply the demand $\dot{Q}_{dis}$. Figure 4.4a and Figure 4.5a show the same situation but are focused on four days only to enable the reader to clearly see how demand is supplied at every hour.

During the summer period a system with a flat plate collector area of 18,319 m², which corresponds to 14 % solar share, cannot supply the demand 100 % at all times. Even though it was dimensioned to meet the demand of July to 100 %, which lasts from hour 4344 till hour 5088, variations in the load and fluctuations in radiation cause a need of additional energy from the CHP plant in the DH main-network.

The additional energy that would be needed in this scenario can be found in Figure 4.2b and Figure 4.3b and accordingly in Figure 4.4b and Figure 4.5b. In Figure 4.2b some longer intervals that do not need additional energy from the DH main-network can already be observed. In these intervals the sub-network operates 100 % independently from the CHP plant and the DH main-network. If the thermal storage is fully recharged every evening, a much greater time interval is free from unregularly additional energy demand that would be needed from the DH main-network. This would require increasing the temperature in the main-network only at the beginning and at the end of the summer season and once daily to recharge the thermal storage.

The thermal storage state of charge and recharging leads to graph c of Figure 4.2 till Figure 4.5. These graphs c show the amount of energy in the thermal storage in red and the amount of energy that the thermal storage is regularly recharged with in blue. As mentioned earlier, only Figure 4.3 and Figure 4.5 show a scenario with a daily recharge of the thermal storage. As this study is not an optimization study about operational management, but an analysis of a system supported by solar heat, the thermal storage recharge was set to 9 pm for every day. Hence the thermal storage is also recharged even if the thermal storage state of charge is large enough to supply the DH sub-network throughout the whole night. In this simulation the recharge of the storage happens throughout the whole year. This is not needed and does not make much sense, because during the winter time the load in the sub-network is that high, that after a recharge of the thermal storage it would discharge nearly in the same time. Outside the summer season, when the DH sub-network is supplied by the CHP plant in the DH main-network, it is more beneficial for the whole system to have fewer changes on the system demand. A daily recharge of the thermal storage would therefore disturb the system in winter more than it would bring benefits.

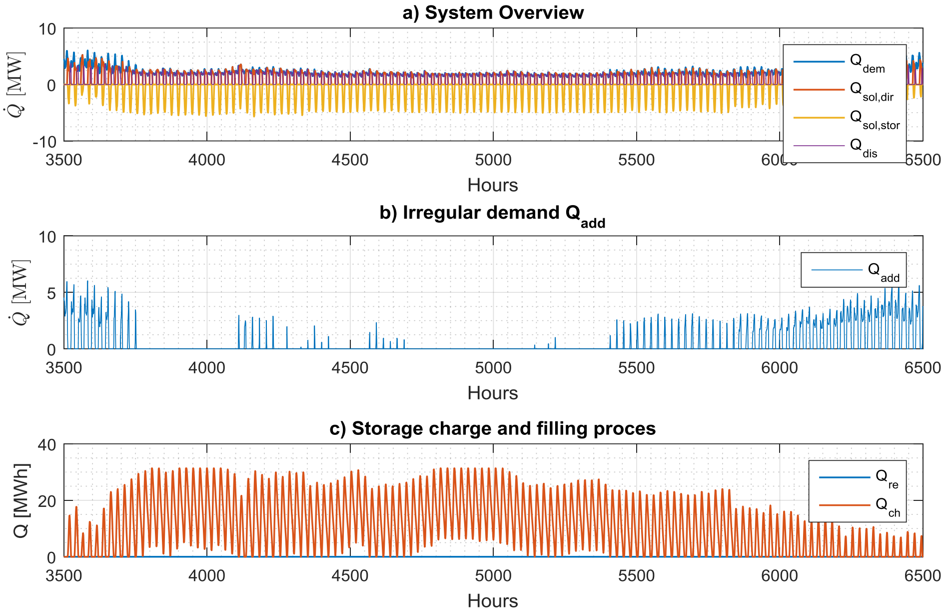

Figure 4.2: Supply and demand curves (a), irregular heat power demand (b) and storage charging (c) during the summer season with 14 % solar share

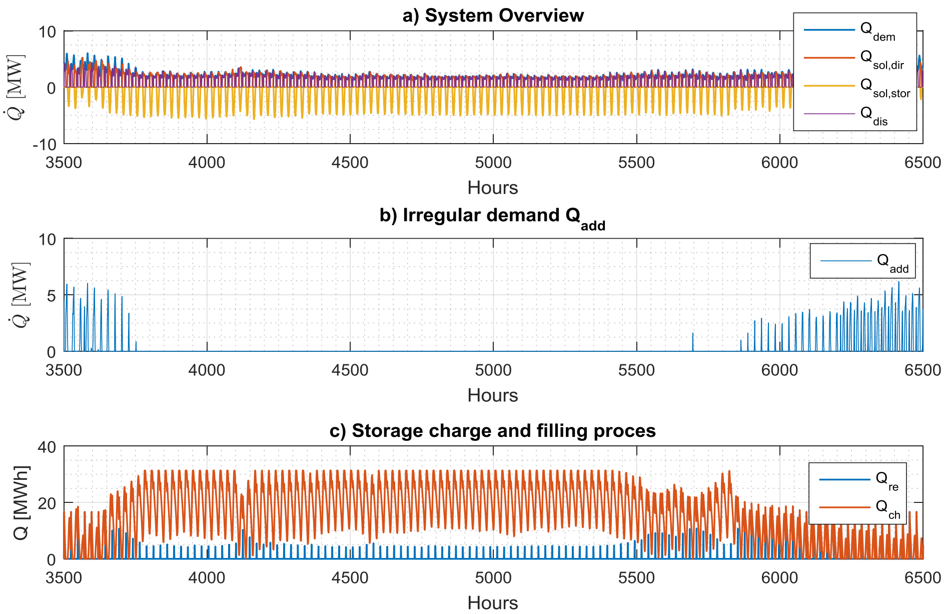

Figure 4.3: Supply and demand curves (a), irregular heat power demand (b) and storage charging (c) during the summer season with 14 % solar share with daily thermal storage recharge

When comparing Figure 4.4*c* and Figure 4.5c it can be observed that the thermal storage state of charge in Figure 4.5c with the evening recharge is more often at its maximum compared to a system without a regular recharge. A higher state of charge brings a larger security that no additional energy during the day is needed from the DH main-network. If the thermal storage is charged too much when good weather or low demand can be expected, it can have the negative result that the storage cannot take up additional solar surplus from the collector field. This decreases the system efficiency as well as not achieving the desired improvement of the CO_2 balance.

While Figure 4.2 and Figure 4.3 display the summer season Figure 4.4 and Figure 4.5 illustrate an excerpt of only four days of the transition time when a collector system can operate close to independency. In these Figures we can inspect in detail how the energy flows are expected to be. The following equation is the base for the relation between the different heat power terms:

$$\dot{Q}_{dem} = \dot{Q}_{sol,dir} + \dot{Q}_{dis} + \dot{Q}_{add} \tag{2.1}$$

The DH sub-network's demand $\dot{Q}_{dem}$ is visible in graphs a as a blue line that is mainly covered by the red line for the direct usable solar energy $\dot{Q}_{sol,dir}$ or the purple line of the thermal storage discharge $\dot{Q}_{dis}$. It can clearly be seen that the solar surplus in yellow, which is placed as negative as it is stored and not used directly, is a continuation of the curve the direct used solar energy starts. At hour 4110, hour 4133 and hour 4160 the demand $\dot{Q}_{dem}$ cannot be covered by direct solar energy and thermal storage discharge. At these hours additional energy from the DH main-network is needed, which can be found in the graphs b.

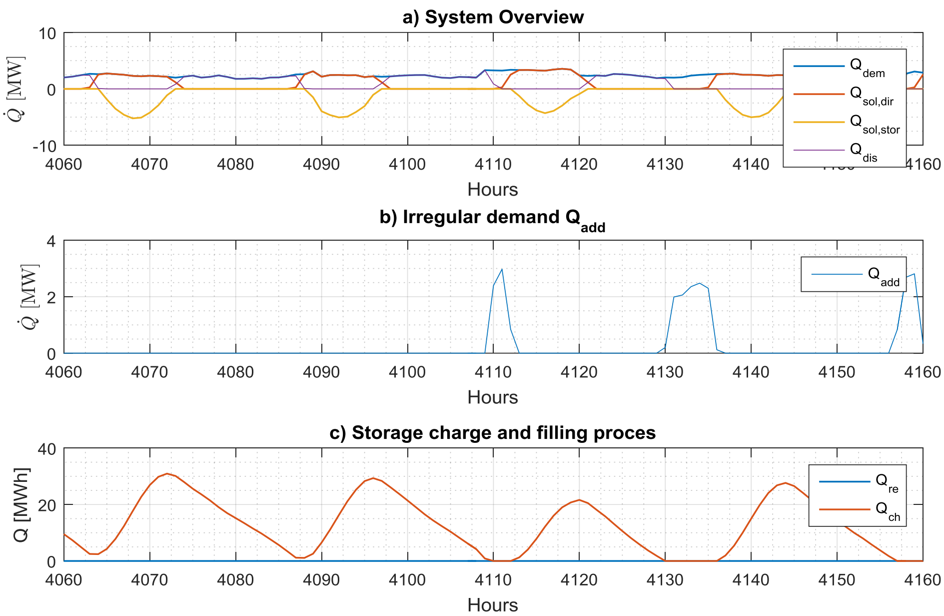

Figure 4.4: Zoomed-in 4 days of supply and demand for the scenario with 14 % annual solar share without regular storage recharge

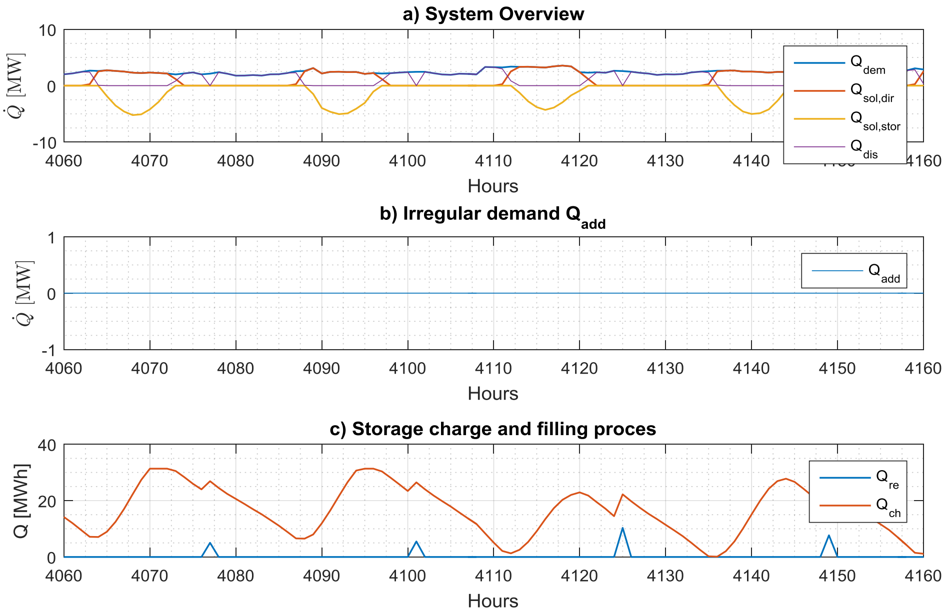

Figure 4.5: Zoomed-in 4 days of supply and demand for the scenario with 14 % annual solar share with daily recharge

Another gap in the supply from the thermal storage or direct solar energy can be found in Figure 4.5a. During the hours that the thermal storage is recharged (4077, 4101, 4125 and 4149, visible in Figure 4.5c) $\dot{Q}_{dis}$ in Figure 4.5a is 0. As the thermal storage is at these times anyways supplied with energy by the DH main-network, also the DH sub-network uses the energy that is sent over.

In Figure 4.5c it can be observed, that the thermal storage is not refilled to its maximum during a recharge of the storage. This can be explained by the different temperature levels in the storage. As explained in Chapter 3.1.5 and 3.1.6 the storage was dimensioned with a temperature difference of 32 K based on 63 °C DH return temperature and a maximum of 95 °C thermal storage temperature. The solar collectors shall deliver 95 °C on days that the thermal storage charge is expected to be above 75 %. The thermal storage recharge from the CHP plant in the DH main-network in the evening is on a temperature level of 80 °C. Therefore, the storage cannot be charged to its maximum level. In such a case a temperature of 95 °C and 80 °C is in the storage. After discharge of the storage additional water with the DH return temperature would enter the thermal storage and add a temperature of 63 °C maximum.

To summarize the main importance of the figures presented in this Chapter, it can be said that a system of the given specification can supply the sub-network's demand during the summer season to a large extent independently of the main-network. If an overnight charging of the storage to 80 °C is given, the irregular demand by the sub-network on the main-network is more predictable. An increase from the presented 14 % solar share to 17.8 % solar share will reduce the need for additional energy supply from the main network during the summer season, but will also increase the losses of solar energy drastically from less than 1 % to about 12 % as the storage is not emptied for the largest part of the summer season. Furthermore, the difference in the collector area between 14 % and 17.8 % solar share is 7,725 m² and will also have a large economic impact.

The optimum system choice is therefore an offset between a system that needs as little additional energy during the summer season as possible with the aim to let the main-network operate as independently as possible and a system that has a collector area as small as possible to reduce system costs as well as to reduce losses during the summer due to storage limitations.

Table 4.1 below lists key parameters of the calculated solutions for a FPC in a best case situation. Regarding CO_2 reduction, it has to be mentioned that the emissions by the CHP plant in the DH main-network were said to be 172 g/kWh. This value multiplied with the annual net solar energy gives the possible CO_2 reduction.

Table 4.1: Calculation results for different annual solar share

Solar share Scenario [%]	**5**	**10**	**100% July**	**15**	**20**
Actual solar share [%]	5	10	14	14.8	17.8
Collector area [m²]	6,507	13,029	18,319	19,536	26,044
Field size [m²]	13,791	27,581	38,808	41,372	55,163
Specific storage volume [l/m²]	7.3	30.3	39.5	40.5	46.2
Storage volume [m³]	50	403	728	802	1,220
CO_2 reduction [t/a]	480	961	1,348	1,424	1,725
Specific solar radiation [kWh/m²a]	429	429	428	423	383

Additional results for ETC can be found in Appendix A.

4.2 Sensitivity Analysis

As explained in Chapter 3.2 it is not possible to compare results calculated in this study directly to the freeware for SDH systems. Therefore, a sensitivity analysis was conducted to visualize different output parameters if the net solar gains are 5 %, 10 %, 15 % and 20 % lower. The results of this study were chosen to be the best case as the used meteorological source gives higher values of solar radiation on the field compared to other meteorological data and thermal losses in the collector field were not included in the calculation. A case of 10 % lower net solar gains is therefore seen as realistic.

In the following the influence on the DH sub-network independence will be graphically presented and the change in the actual solar share, the CO_2 reduction and the specific thermal energy costs will be listed in a table.

The influence on the independence of the DH sub-network in the summer season is rather case specific. Assuming that the solution of a regular recharge is chosen, Figure 4.3 can be compared with the excerpt of the additional demand with 10 % and 15 % reduced solar net gains in Figure 4.6 and Figure 4.7 respectively.

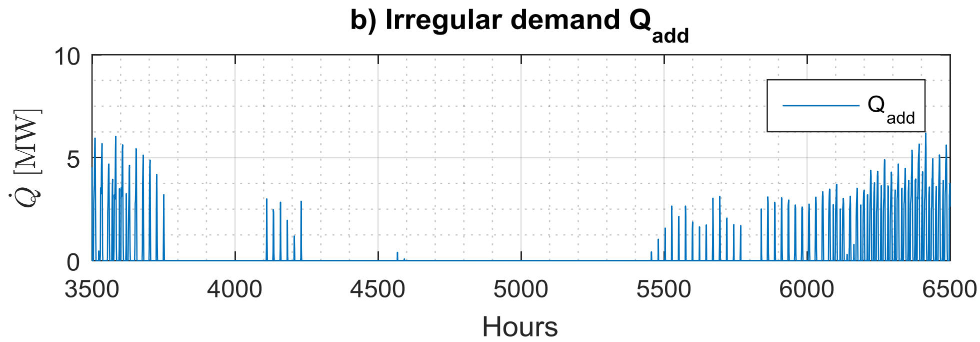

Figure 4.6: Additional demand from the DH main-network for 10 % less net solar gains

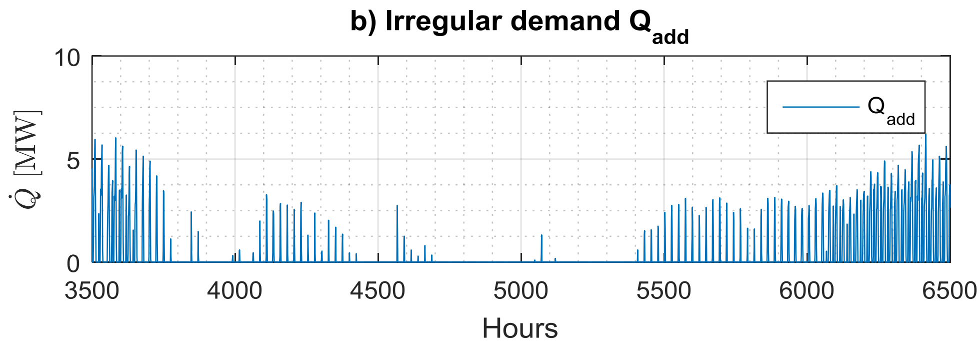

Figure 4.7: Additional demand from the DH main-network for 15 % less net solar gains

Between Figure 4.6 to Figure 4.7 an increase of additional irregular demand within the summer season can be observed. When comparing the two figures to Figure 4.2b, the “best case” without a regular storage recharge, a similarity of occurring hours with additional heat can be observed. Therefore, a storage designed to take up the solar surplus of a day in southern Germany with a regular recharge can achieve a DH main-network independence improvement of about 10 % to 15 %. The independence improvement is, that the main network can operate for a longer time during summer on an independent temperature level from the sub-network.

A final decision in which scenario a system is independent enough can only be made if the exact benefits for the CHP plant's and the DH main-network's independence are known. Part of these benefits are the possible reduction of the DH supply temperature in the DH main-network and thereby the increased efficiency of the CHP plant. The decreased DH system temperatures would also result in decreased thermal losses. Additionally, key parameters as annual CO_2 reduction and the resulting reduction of the PEF factor can massively influence a decision. If energy generation costs are too high, it might be more feasible to operate the whole DH network on higher system temperatures instead of investing in a SDH plant. Finally, also the reduced CO_2 emissions that have a positive impact on the PEF can be of great importance. Especially the implications of a decreased PEF value of a system are very dependent on the country, due to different legal regulations.

To compare the values mentioned, Table 4.2 lists an overview of key parameters of the sensitivity analysis. Within this sensitivity analysis the collector area of 18,319 m² has remained the same but the net solar gains have been reduced by values from 0 % to 20 % in steps of 5 %. A reduction of the actual solar share and CO_2 emission can be expected whereas the cost for thermal energy increases.

Table 4.2: Sensitivity analysis of the 100 % July Scenario

Scenario: 100 % July, with lower net solar gains [%]	**0.00**	**5.00**	**10.00**	**15.00**	**20.00**
Actual solar share [%]	14.03	13.37	12.66	11.96	11.26
Specific solar gains [kWh/m²a]	427.8	407.6	386.2	364.7	343.3
CO_2 reduction [t]	1347.9	1284.3	1216.8	1149.2	1081.6

4.3 Financial Analysis

In this Chapter a financial analysis is performed. The investment discounting are performed according to the VDI 2067 Part 1 (VDI-Gesellschaft 2000) and is similar to the SDH Online-Calculator and the financial analysis in Pauschinger (2015). The investment was discounted over 25 years with an interest rate of 4 %. The results in this case can only be taken as estimations for costs because additional costs besides the main components like collectors, storage and the price of land were added in percentage on the main investment costs. The additional costs taken into account are:

Control technology	3 %
System technology	7 %
Construction works/ building	1 %
Planning	10 %
System integration	5 %

Source: (Schmidt & Deschaintre 2013)

The thermal storage specific costs used are 140 €/m³ (Maripuu & Dalenbäck 2011). Costs of land were given by the utility company that operates the example networks of this report. It was calculated at 9 €/m² land. As the costs of land are taken separately the building and area costs in (Schmidt & Deschaintre 2013) are here only used as Construction works/ Building and account for 1 %. The collector costs used for the feasibility analysis are 200 €/m² for the FPC (Trier 2015). The costs for the ETC of 340 €/m² were given by Ritter XL in 2012 and used in (AGFW 2013).

Additionally, funding was assumed for the project. As explained in Chapter 2.3, 40 % of the capital costs for the collector area and 30 % of the thermal storage capital costs are assumed to be funded.

The maintenance and operation cost were added in form of percentages on the initial investment fractions:

Control technology	2.5 %
System technology	2.25 %
Construction works/ building	2 %
Thermal storage	1.25 %
Collectors	1 %

Source: (Schmidt & Deschaintre 2013)

Figure 4.8 and Figure 4.9 visualize the relation of FPC and ETC between annual costs and the annual CO_2 reduction in Figure 4.8, and specific heat generation costs and the collector area in Figure 4.9. In both Figures an increase in slope can be observed at some point. From the point on where the slope increases, the tipping point, the surplus heat cannot be stored completely because the thermal storage is not emptied overnight and will be filled to its maximum faster. In order to store energy for longer periods, a larger specific thermal storage size is needed. If the specific storage volume would be larger this tipping point would appear at larger system sizes – in the graphics the tipping point would move to the right. With a larger thermal storage, the system could store heat over longer periods than only one day (in this study it was dimensioned for intraday energy storage). Seasonal storages can, according to the SDH Online-

Calculator, have a specific thermal storage size up to 60 times the size of a short term storage.

The top point of each line in both figures in this chapter represents a scenario that aims for 20 % solar share and the lowest point of each line represents 5 % solar share. The lines look the same if instead of Annual CO_2 reduction the net solar gain is placed on the x-axis, due to the linear relationship between both.

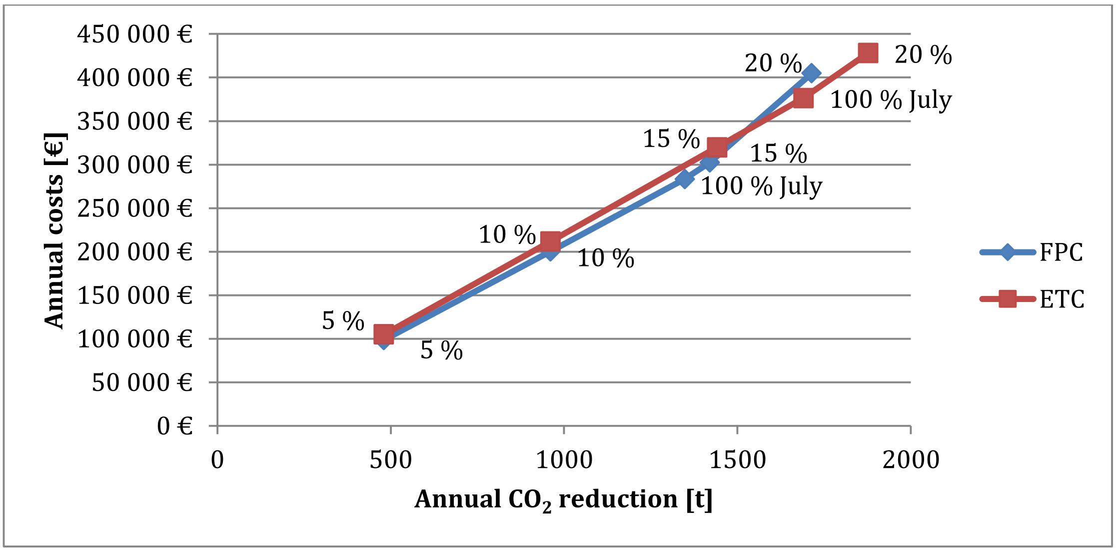

Figure 4.8: Annual costs per CO_2 savings

The phenomenon of the tipping point is better visible in Figure 4.9. The figure displays the cost difference of both systems to achieve the same solar share at different field sizes. Despite of a scenario that aims for a solar share of 20 % the FPC systems have lower specific heat generation costs. This difference in costs would decrease if the specific land costs rise, because the FPC systems need a larger collector area to achieve the same solar share.

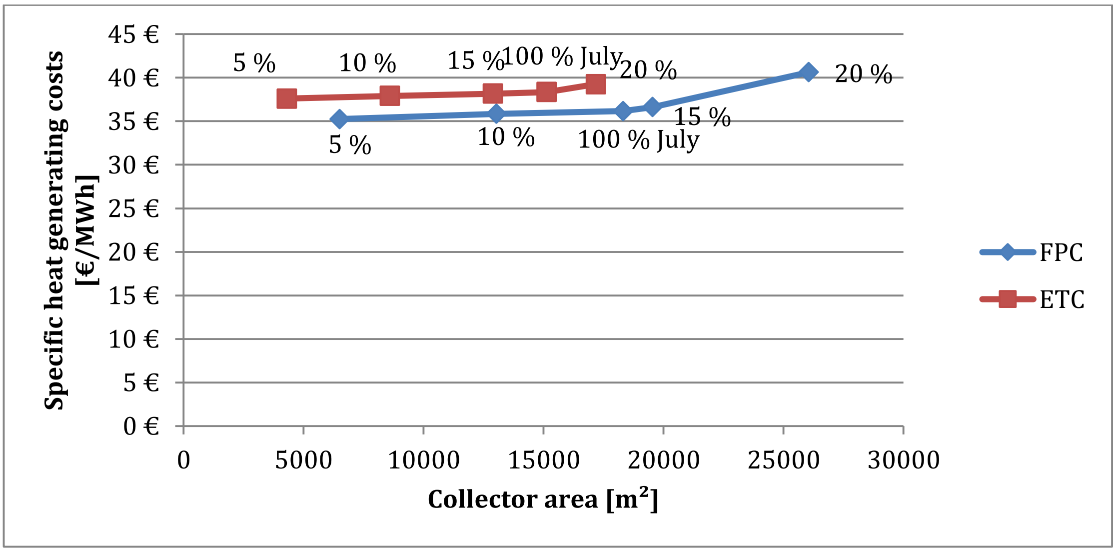

Figure 4.9: Specific heat price per collector area

In this feasibility study the economy of scale is not considered. For the thermal storage as well as the collector area a fixed price was used. If higher prices for smaller systems are assumed, it can be expected that Figure 4.9 will have a curve with the lowest point at a system size larger than 5 % solar share, because specific costs would decrease with increasing system size.

In Table 4.3 the main economical parameters are listed. The interest rate used was 4 % and the costs were discounted over 25 years. The listed values in Table 4.3 as well as the figures are under consideration of Chapter 2.3 explained funding possibilities in Germany.

Table 4.3: Overview of key economical parameters

Solar share scenario	**5 %**	**10 %**	**100 % July**	**15 %**	**20 %**
Collector area [m²]	6,508	13,029	18,319	19,536	26,044
Usable solar heat [MWh]	2,793	5,587	7,837	8,260	9,964
Total capital investment [€]	1,305,330	2,653,754	3,753,284	4,005,917	5,360,678
Annual costs [€/a]	98,473	200,325	283,386	302,473	404,825
Heat price [€/MWh]	35.25	35.86	36.16	36.62	40.63
CO_2 savings [t]	480	961	1,348	1,421	1,714
Specific CO_2 saving cost [€/tCO2]	204.96	208.48	210.24	212.90	236.23

5 Discussion and Conclusion

In this chapter the presented work is discussed and a conclusion of the is taken. Methods and results of the project are summed up and weaknesses are discussed. Furthermore, the applicability of the work is shown and a connection to other and future research is made.

5.1 Discussion

In the presented work a new methodology is shown that is based on general numerical tools as MATLAB. It uses given load curves and weather data to dimension a SDH plant. With this method and software like MATLAB, results can be analysed and visualized to implicate benefits of a SDH plant for the overall system. As presented in chapter 4 a benefit can be that DH network parts can be separated from the DH main-network for some time during the year, which enables to operate them on different temperature levels at these times.

The calculation methodology for this project was based on energy flows instead of specific mass flow, temperature levels and specific heat capacity of the collector fluid, which is a simplification that also reduces risk of wrongly assumed values. Not calculating every parameter of the collector field also avoided the question how the field should be operated in the calculation, either with a constant flow or a constant temperature.

Despite the simplified calculation pattern the methodology used has proved detailed enough to point out possible benefits for the overall DH network. These benefits were described in the chapter results. There, a predicted CO_2 reduction as well as the reduced demand on the DH main-network during the summer months was presented. Furthermore, a sensitivity analysis was performed to estimate changes in the results if the net solar gains are not as large as expected after the calculation.

With this project we can confirm Meißner et al. (2012) who criticise overdimensioning of solar thermal storages. In good agreement with (Meißner et al. 2012) the calculated specific storage volume was in the calculated scenarios up to 20 % solar share below 50 l/m² which is the lowest selectable value in the SDH Online-Calculator. However, the storage only accounts for a small percentage of the total investment. Additionally, the project results display the possibility of operating a DH sub-network during the summer months independently for some time. If a thermal storage of the SDH plant is also recharged regularly, the energy needed from an additional heat source can be supplied in predictable intervals from the CHP plant in the DH main-network. This avoids including a back-up boiler that may have a lower efficiency and worse effect on the PEF than using energy from the existing centralized CHP plant.

Furthermore, this project addresses a potential use of large scale solar heating systems in CHP plant based systems that was not yet discussed in other literature. So far SDH was either used as an additional energy source when the CHP plant was not large enough to supply the whole DH network or when the buildings' structure in a district changes and thereby enables lower temperatures compared to the rest of the system. In contrast, this project points out that SDH can supply parts of a DH network with slightly higher temperatures to improve the performance of a CHP plant by enabling the DH main-network to operate on lower temperatures, which can increase the CHP plants' efficiency.

The study shows that the accuracy of dimensioning a solar district heating system highly depends on the quality of the input data used. Calculations on the basis of annual data provide a rough idea on the necessary collector area and storage volume for a given heat demand. However, exact dimensioning can only be done by using hourly-values of solar radiation and heat load for a whole year period.

The methodology for the integration of solar heat into DH systems that is presented in this report leads to more detailed results and avoids overdimensioning of storage volume, compared to freeware tools.

The example calculation shows that a solar thermal DH sub-network with an annual solar share of about 14 % in case of a FPC can be realised without an auxiliary gas or biomass boiler, if a storage with recharging option is given. During the summer months the solar heat gains cover the total heat demand of the network whereas in other times of the year the main-network provides the additional heat. For this system short-term storage with a specific thermal storage volume below 40 l/m² is sufficient.

Due to lack of operational possibilities of the CHP plant and the efficiency improvements of the CHP plant in case of lower system temperatures the economic benefits of a SDH plant can only be calculated to a limited extend. Further research on the side of the CHP plant are needed in order to give more detailed economical values.

When the results of the presented work were compared to other calculation methods and tools some differences were noted:

Firstly, the irradiation on the collector field imported from PVGIS differed about 10 % from values visible in the SDH Online-Calculator for the same location, which is based on radiation values from Meteonorm.

Secondly, heat losses in the piping system and the storage of about 5 % to 10 % were added as part of the sensitivity analysis and not in the main calculation.

Thirdly, results of expected CO_2 savings differ in this project compared to the SDH Online-Calculator, because a CO_2 emission factor of 172 g/kWh was given for the CHP plant considered in this project.

5.1.1 Limitation of the Matlab code

Besides the more general issues the calculation in this study neglects a range of details that would influence the results to some extent. Some of the details could be included in the calculation code but would require higher efforts. Other details e.g. shading of the collectors can have a big influence. Due to a lack of information about the site, shading could not have been taken into account. Below is a list of some unconsidered details that would influence the system efficiency:

- exergy losses due to loss of stratification in the thermal storage
- solar radiation values from PVGIS are based on hourly values for an example day of each month and not on hourly values for a whole year.
- storage recharge time was set to 9 pm every day.

- the storage recharge happens within 1 hour, limitations in e. g. volume flow are not taken into account.
- collector field size is based on a factor calculated with the collector size and angle to calculate a row distance.
- collector outlet temperature outside of the summer season is equal to DH supply temperature.
- calculated costs are based on experienced values in other projects.
- technical requirements and physical changes when using a system that uses a glycol-water mixture in the collector field.

With the presented issues further research on the example case but also in general in the field of applying large solar thermal systems in existing DH systems seems to be needed.

A comparison of the results of this methodology should be further verified with a similar calculation with software that is commonly used to dimension solar thermal plants and also with a different source of meteorological data. Additionally, for the given example case the performance of the CHP plant and the actual influence on its efficiency would be of interest if the DH temperatures in the main-network can be lowered by a few Kelvin.

Furthermore, also due to the aim of reducing fossil fuels, more research is needed in how far SDH can play a role here and when it is to be introduced into large systems most feasibly to allow a smooth transition to alternative more renewable heat sources. The focus of research of SDH systems so far was rarely on large scale CHP systems, even though these will also have to change in the future.

Focussing on Germany, the funding for CHP produced energy has a large impact on feasibility and thereby interest in SDH in large CHP based DH systems. Only stronger regulations for new low energy consuming buildings that require a low PEF may increase the importance of SDH in such systems.

The political development, not only in Germany, therefore has a strong influence on the development of SDH in combination with CHP plants.

5.2 Conclusion

The integration of solar heat into existing DH systems brings benefits to a fossil CHP plant based system such as CO_2 reduction, primary energy factor improvement and operational flexibility. In the given case a system with FPC which supplies about 14 % solar share and a thermal storage of 728 m³ delivered the best results. The possibility to supply a sub-network for certain periods of the year by solar heat, allows the CHP plant in the main network to operate with higher efficiency at times that the DH main-network temperatures can be lowered compared to those of the sub-network.

Currently the cost for heat from SDH systems in comparison to CHP plant based heat may be higher in some cases, though other factors such as system flexibility and ecological aspects may still rule the decision over a possible investment.

References

AGFW, 2010. *AGFW-Arbeitsblatt FW 309 Teil 1*, Frankfurt am Main.

AGFW, 2013. *Transformationsstrategien Fernwärme*, Frankfurt am Main.

BDEW, 2013. *Umsetzungshilfe zum Kraft-Wärme-Kopplungsgesetz – KWK-G*, Berlin. Available at: http://www.bdew.de/internet.nsf/res/07FB721D9C0144E8C1257BF1003FF133/ $file/KWK-G Umsetzungshilfe f?r Netzbetreiber 2.0_final.pdf.

Berberich, M. et al., 2015. *SOLAR-KWK Entwicklung multifunktionaler Systeme zur solar unterstützten Kraft-Wärme-Kopplung – solare Fernwärme und saisonale Wärmespeicher für die Energiewende*, Stuttgart.

Le Denn, A., 2013. *Solar district heating guidelines Calculation tools and methods*, Perpignan.

European_Commission, PV GIS. Available at: http://re.jrc.ec.europa.eu/pvgis/apps4/pvest.php# [Accessed May 10, 2016].

Fisch, M.., Guigas, M. & Dalenbäck, J.-O., 1998. A review of large-scale solar heating systems in Europe. *Solar Energy*, 63(6), pp.355–366. Available at: http://www.sciencedirect.com/science/article/pii/S0038092X98001030.

Frederiksen, S. & Werner, S.E., 2013. *District heating and cooling*, Lund: Studentlitteratur.

Kovacs, P., 2012. *A guide to the standard EN 12975*, Borås.

Lubinski, B., 2014. *EnEV und Fernwärme*, Frankfurt am Main.

Maripuu, M. & Dalenbäck, J.-O., 2011. *SUNSTORE 4 WP5 - European level concept study Feasibility / simulation studies*, Göteborg.

Meißner, R., 2016. Die Suche nach dem (wirtschaftlichen) Optimum Teil 1. *Heizungsjournal*, 1.

Meißner, R. et al., 2012. Sinn und Unsinn von Solarspeichern. *FEE Heizungsjournal - Special*, pp.1–6.

Pauschinger, T., 2015. *Solnet BW Solare Wärmenetze für Baden-Württemberg Grundlagen | Potenziale | Strategien*, Stuttgart.

Schmidt, T. & Deschaintre, L., 2013. SDH online-rechner.

Solites, 2015. SDH. Available at: www.solar-district-heating.eu.

Trier, D., 2015. Solare Fernwärme in Dänemark - Entwicklungen und Trends. *Erneuerbare Energie*, 3. Available at: www.aee.at/aee/index.php?option=com_content&view=article&id=870&Itemid =113.

Urbaneck, T. et al., 2015. Solar District Heating in East Germany – Transformation in a Cogeneration Dominated City. *Energy Procedia*, 70, pp.587–594. Available at: http://www.sciencedirect.com/science/article/pii/S1876610215002866.

VDI-Gesellschaft, 2000. *VDI 2067 Part 1 Economic efficiency of building installations Fundamentals and economic calculation*, Düsseldorf.

Appendix A: Results of Ritter XL collector

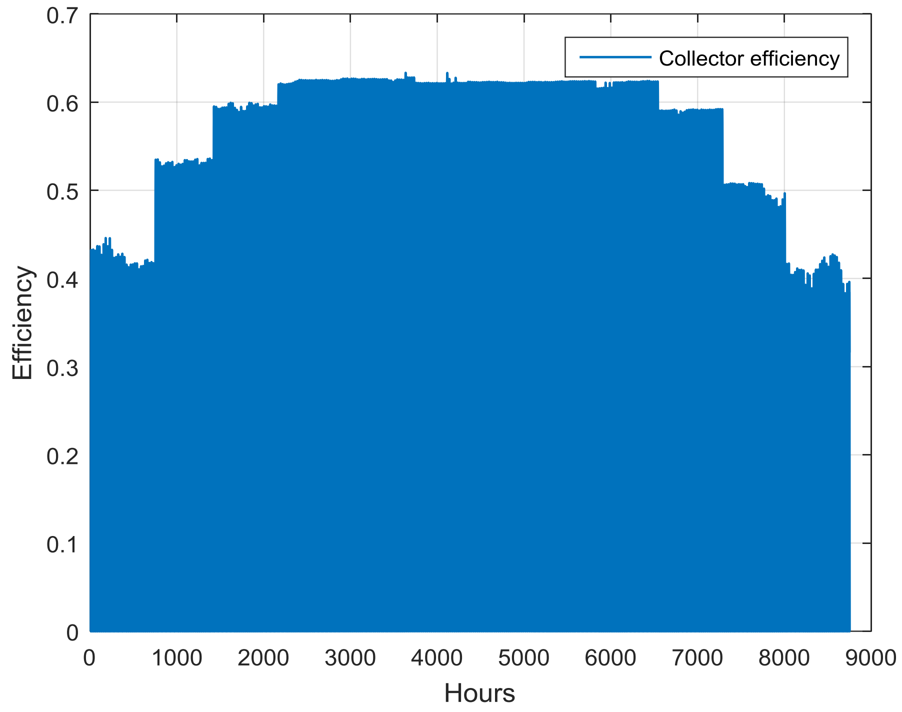

Figure 0.1: Hourly collector operation point efficiency for an example year

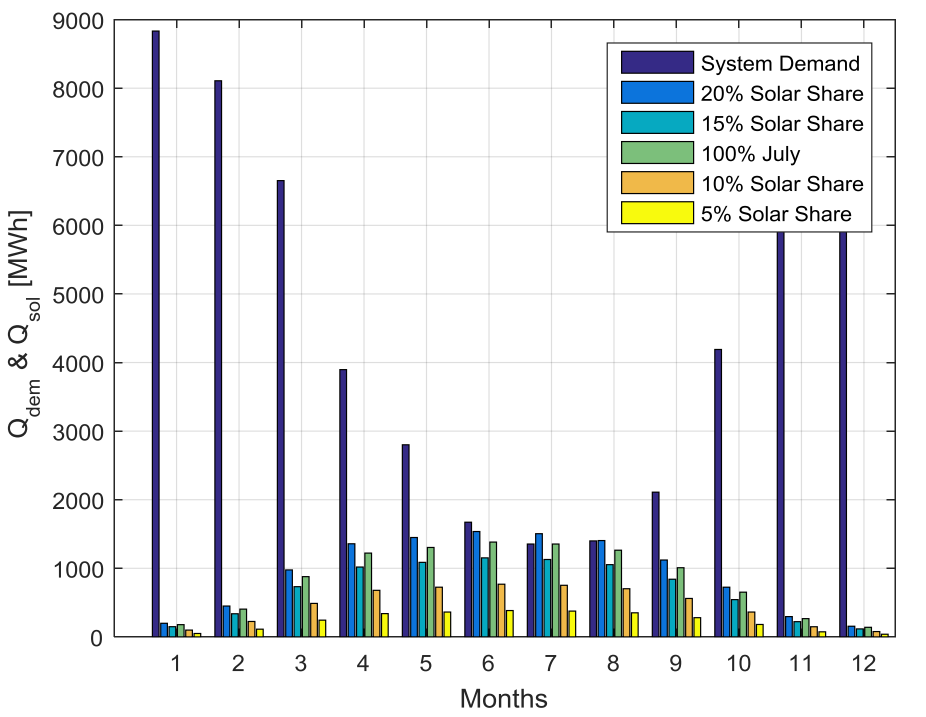

Figure 0.2: Net solar gain compared to demand for different solar share variations

Table 0.1: Calculation results for different annual solar share

Solar share [%]	**Actual solar share [%]**	**Collector area [m²]**	**Field size [m²]**	**Specific storage volume [l/m²]**	**Storage volume [m³]**
5	5	4,297	13,756	1.3	6
10	10	8,588	27,511	21.2	182
15	15	12,885	41,267	37.6	478
100 % July	17.6	15,124	48,442	43.5	647
20	19.5	17,176	55,023	47.4	801

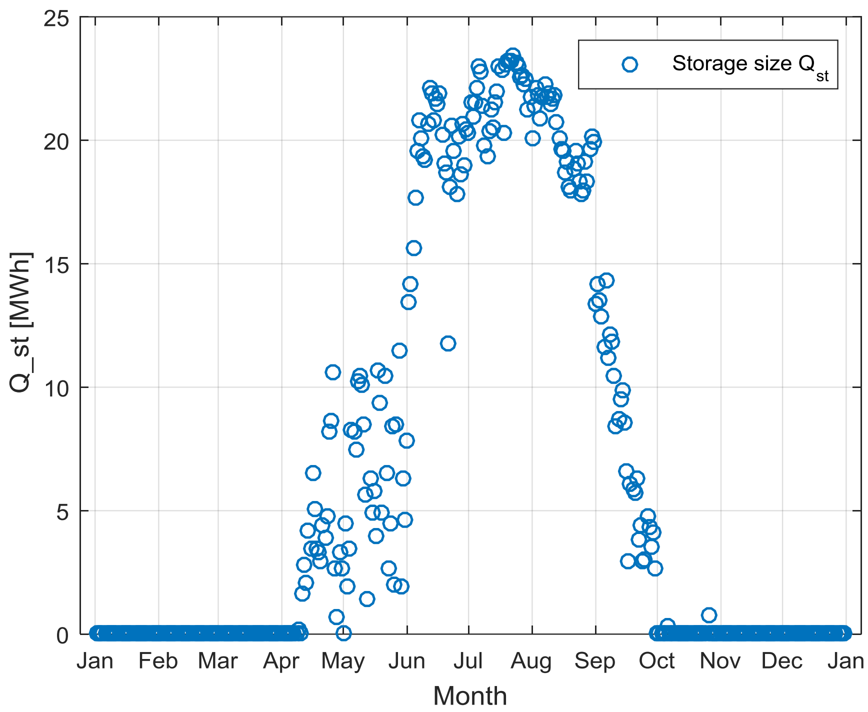

Figure 0.3: Needed storage capacity to store solar surplus energy for an annual solar share of 14 %

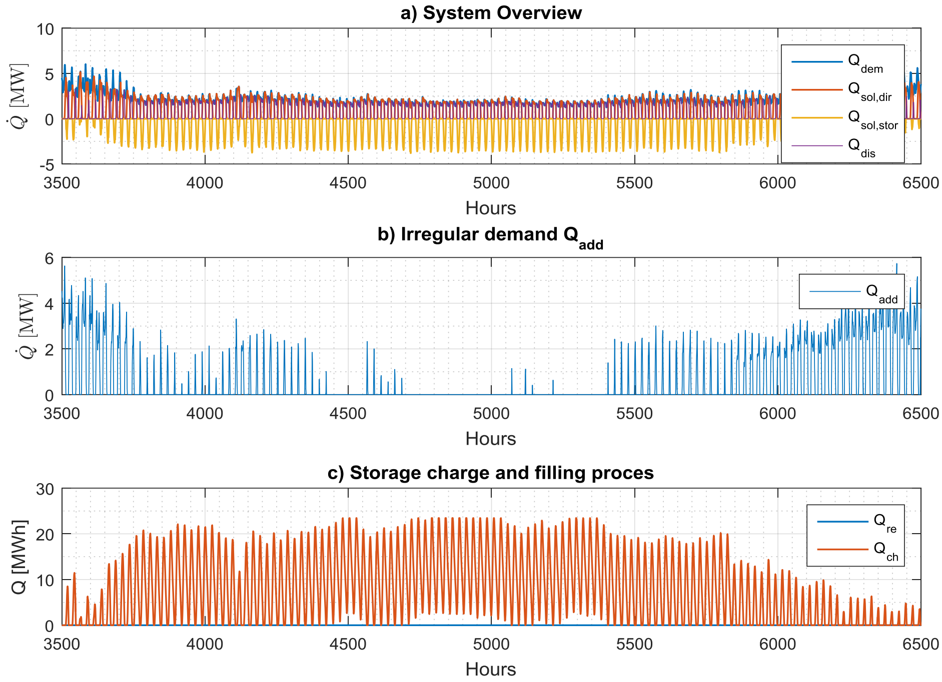

Figure 0.4: Supply and demand curves (a), irregular heat power demand (b) and storage charging (c) during the summer season with 14 % solar share

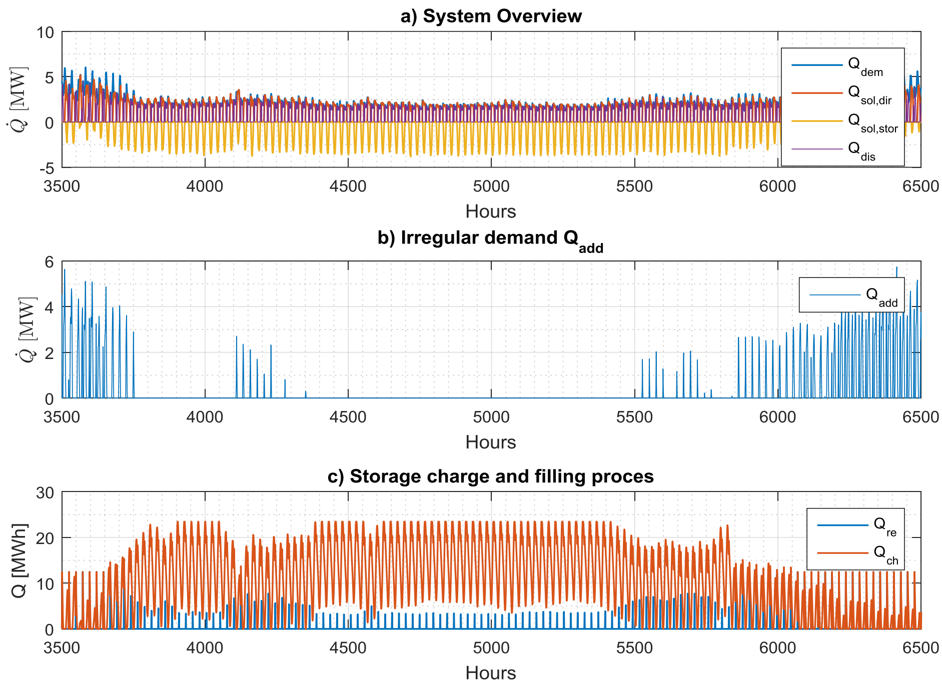

Figure 0.5: Supply and demand curves (a), irregular heat power demand (b) and storage charging (c) during the summer season with 14 % solar share with daily thermal storage recharge

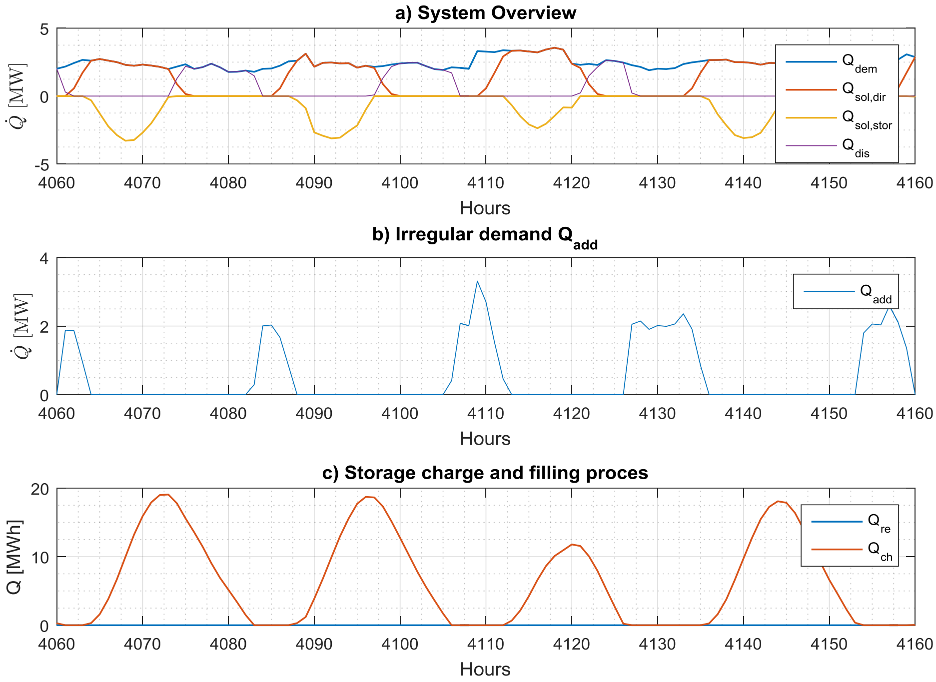

Figure 0.6: Zoomed in 4 days of supply and demand for the scenario with 14 % annual solar share, without regular storage recharge

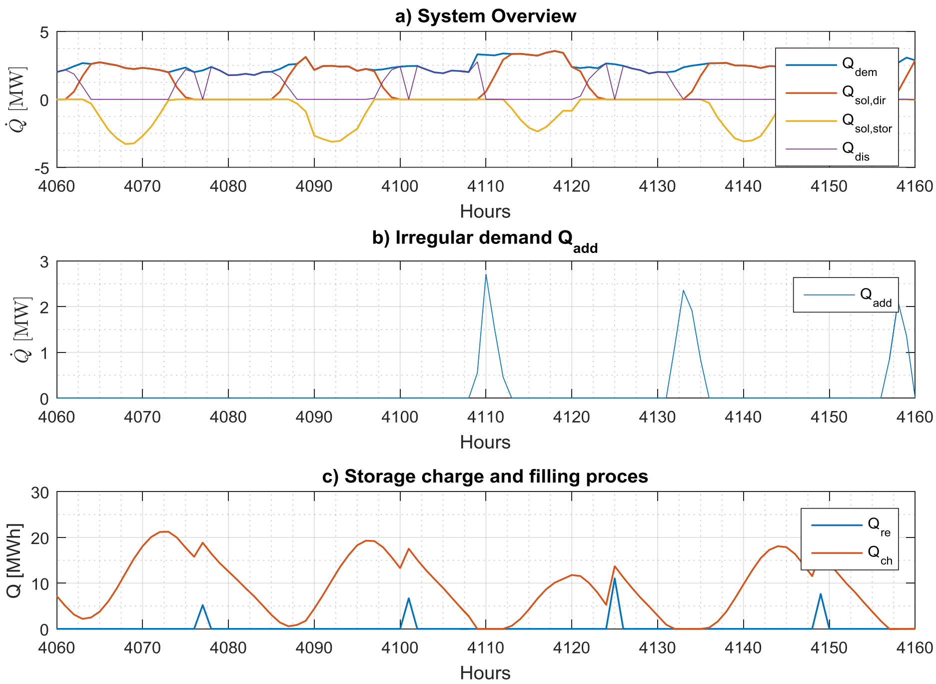

Figure 0.7: Zoomed in 4 days of supply and demand for the scenario with 14 % annual solar share, with daily recharge

TABLE OF RESULTS OF THE BEST CASE

Table 0.2: Calculation results for different annual solar share

Solar share [%]	**5**	**10**	**15**	**100 % July**	**20**
Actual solar share [%]	5	10	15	17.6	19.5
Collector area [m²]	4,297	8,588	12,885	15,124	17,176
Field size [m²]	13,756	27,511	41,267	48,442	55,023
Specific storage volume [l/m²]	1.3	21.2	37.6	43.5	47.4
Storage volume [m³]	6	182	478	647	801
CO_2 reduction [t/a]	480	961	1,441	1,69	1,877
Specific solar radiation [kWh/m²a]	671	671	671	669	655

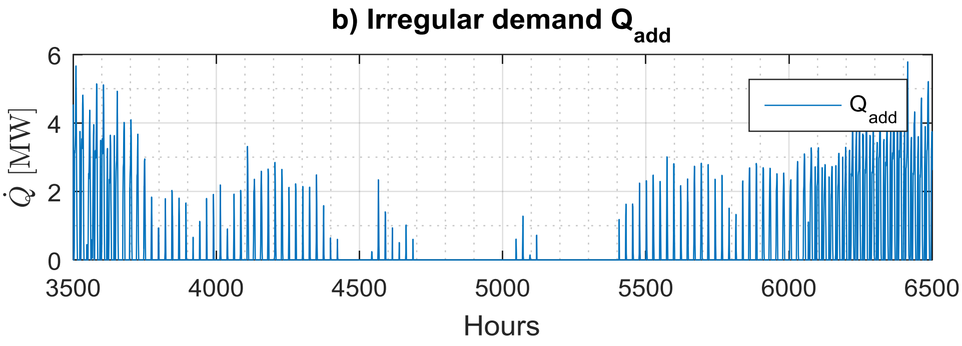

Figure 0.8: Additional demand from the DH main-network for 10 % less net solar gains

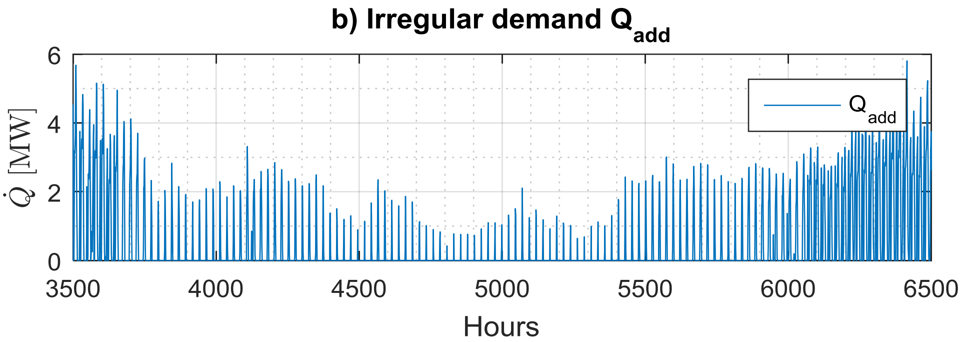

Figure 0.9: Additional demand from the DH main-network for 15 % less net solar gains

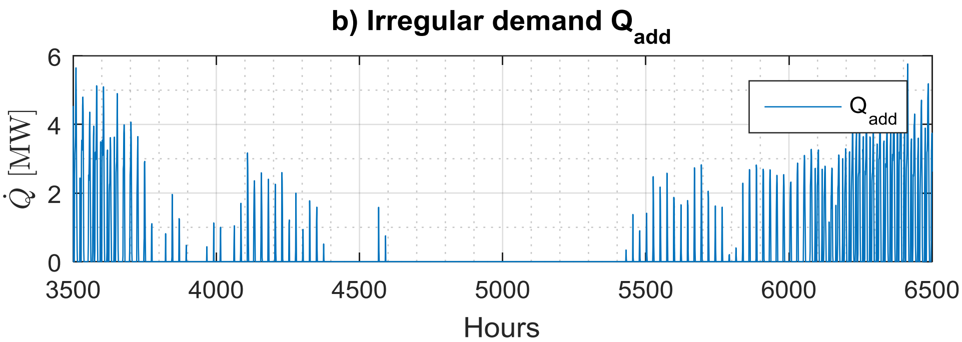

Figure 0.10: Additional demand from the DH main-network for 15 % less net solar gains with a 20 % solar share system

Table 0.3 Sensitivity analysis of the 100 % July Scenario

Scenario: 100 % July with % loss of net solar gains	**0**	**5**	**10**	**15**	**20**
Actual solar share [%]	17.6	16.8	15,87	15.0	14.1
Specific solar gains [kWh/m²a]	669	637	604	570	537
CO_2 reduction [t]	1690	1610	1525	1440	1356

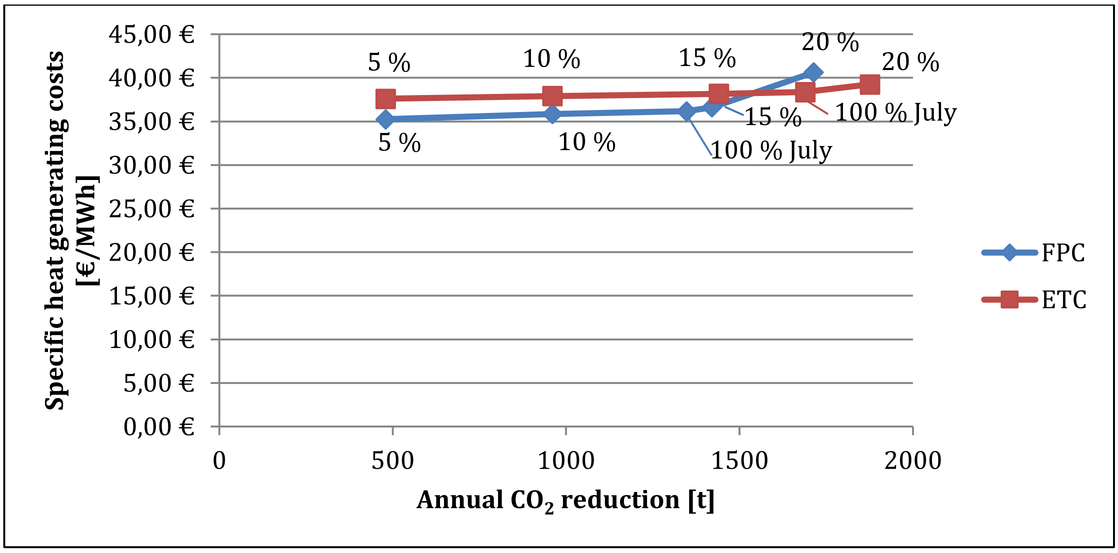

Figure 0.11: Investment costs per CO2 savings

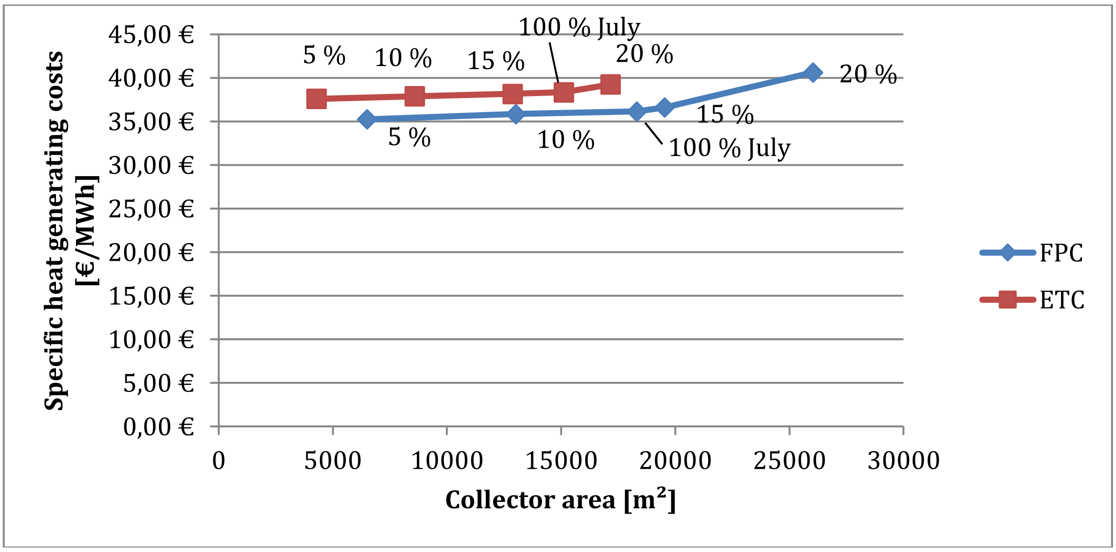

Figure 0.12: Specific heat price per solar share

Table 0.4: Overview of key economical parameters

Solar share [%]	**5 %**	**10 %**	**15 %**	**100% July**	**20 %**
Collector area [m²]	42296	8588	12885	15124	17176
Usable solar heat [MWh]	2793	5586	8380	9811	10907
Total capital investment [€]	1,380,939	2,783,260	4,203,240	4,945,157	5,625,175
Annual costs [€]	105,042	211,763	319,869	376,356	428,130
Heat price [€/MWh]	37.60	37.91	38.17	38.36	39.25
CO2 savings [t]	480	961	1441	1690	1877
Specific CO2 saving cost [€/tCO2]	218.63	220.38	261.12	189.24	228.09

Appendix B: Collector datasheets

ARCON Solar Collector
Type HT-HEATboost 35/10

Datasheet page 2/2

Casing features
Welded aluminum frame and back plate
Air vents to reduce moisture accumulation

Absorber

Type:	Selektive - Tinox
Absorption/Emission	α > 0,95/ε < 0,05
Material:	Copper pipes/aluminum plates
Pipe System:	18xØ10 parallel pipes and 2xØ35 distribution pipes
Absorber plate thickness:	0,5 mm

Insulation

Back side:	75 mm mineral wool
Side:	30 mm mineral wool

Cover

Numbers:	1
Material:	Anti reflex glass (AR)
Thickness	3,2 mm

Connections
Stainless steel flex hose with compression fittings: 2 x 35 mm

Pressure rating

Max working pressure:	10 bar
Test pressure:	14,3 bar
Recommended flow:	0,2-5 m^3/h

Collector inclination angle

Recommended	25-60°

Figure 4: Sectional cut of the HT-HEATstore collector

Figure 5: Stainless steel flex hose mounted on collectors

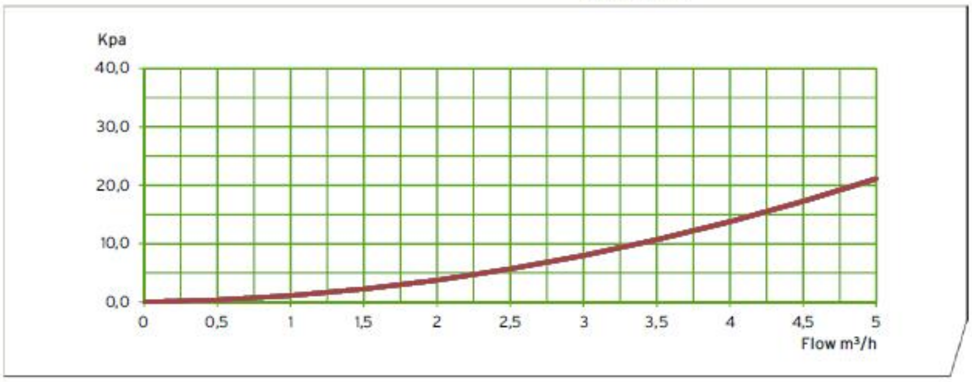

Figure 5: Pressure loss curve incl. one hose

HT_HEATboost_35-10_ENG_REV003

ARCON SOLAR

ARCON Solar A/S / Skørping Nord 3 / DK-9520 Skørping / Tel. +45 98 39 14 77 / arcon@arcon.dk / www.arcon.dk

Figure 0.13: Datasheet Source: Arcon Sunmark

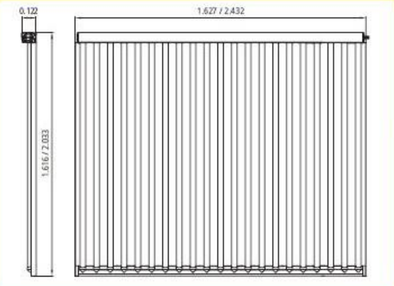

Evacuated Tube Collectors XL P Series

- Highly Efficient Evacuated Tubes based on the Thermos Flask Principle (Dewar Tubes)
- Antireflective Coating
- Weather-Proof CPC Reflector (Compound Parabolic Concentrator)
- U-Shaped Pipe, Material: Copper
- Designed for Very Large Systems and Industrial Applications

Technical Specifications

Series		XL 15/26 P	XL 15/39 P	XL 19/33 P	XL 19/49 P
Number of evacuated tubes		14	21	14	21
η_0 (aperture), DIN 4757-4 or EN 12975	%	68.7	68.7	68.7	68.8
a_1 with wind, in relation to aperture	W/(m²K)	0.613	0.613	0.613	0.583
a_2 with wind, in relation to aperture	W/(m²K²)	0.003	0.003	0.003	0.003
$K_{\theta,trans}$ (50°), in relation to aperture		0.96	0.96	0.96	0.96
$K_{\theta,long}$ (50°), in relation to aperture		0.90	0.90	0.90	0.90
Modular dimensions (length x width x depth)	m	1.616 x 1.627 x 0.122	1.616 x 2.432 x 0.122	2.033 x 1.627 x 0.122	2.033 x 2.432 x 0.122
Gross surface area	m²	2.63	3.93	3.31	4.94
Aperture area	m²	2.33	3.49	3.00	4.50
Collector content	Liter	2.13	3.19	2.53	3.79
Weight	kg	41	64	49	72
Max. permitted operating pressure	bar	10	10	10	10
Stagnation temperature, max.	°C	338	338	338	338
Connection distance, compression fitting	mm	15	15	15	15
Collector material		Al / Steel / Cu / glass / silicone[1] / PBT / EPDM / TPE			
Glass tube material		borosilicate glass 3.3			
Selective absorber coating material		3 Target			
Glass tube, (Ø ext./Ø int./wall thickn./tube lgth.)	mm	47/36.2/1.6/1920			
Colour (aluminium frame profile)		aluminium grey (natural anodised / A6CO)			
Colour (plastic parts)		black			
Test report EN 12975-2	ITW test number	11COL1008/2OEM02	11COL1008/2OEM02	11COL1008/2OEM02	11COL1007/1OEM02
DIN CERTCO registration number	Solar KEYMARK	011-7S2434R	011-7S2434R	011-7S2434R	011-7S2425R
Heat transfer medium		water			

[1] Silicone free version on request

Characteristics at Various Irradiations

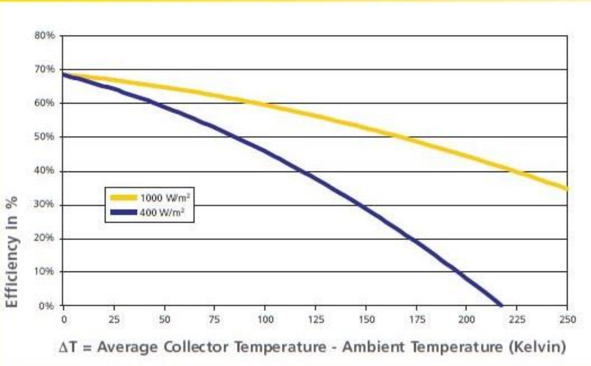

Ritter XL Solar GmbH
Ettlinger Str. 30
76307 Karlsbad
Germany
Tel. +49 7202 922-254
Fax +49 7202 922-125
info@ritter-xl-solar.com
www.ritter-xl-solar.com

Figure 0.14: Datasheet Source: Ritter XL